American Psychology Association, 6th ed.

ABSTRACT

Title of Document: EVALUATION OF CURCUMIN-LOADED NANOLIPOSOMES FOR THE TREATMENT AND PREVENTION OF AGE-RELATED MACULAR DEGENERATION

Sriramya Ayyagari, Haris Dar, Vivian Morton, Kevin Moy, Chadni Patel, Lalithasri Ramasubramanian, Nivetita Ravi, Samantha Wood, Andrew Zhao, Melanie Zheng, Kiet Zhou

Directed by: Dr. Jose Helim Aranda-Espinoza
Associate Professor, Fischell Department of Bioengineering
University of Maryland, College Park

Age-related macular degeneration (AMD), the most common cause of vision loss for people age 50 and over, is a disease characterized by the buildup of oxidative stress in the back of the eye. Current remedies are limited to intravitreal injections that only target the more severe 'wet' form; the common 'dry' form has no readily available pharmaceutical solution. Curcumin, a natural antioxidant found in the Indian spice turmeric, has shown potential in combating inflammatory diseases like AMD; however, the molecule also demonstrates poor bioavailability. This research aimed to create curcumin-loaded nanoliposomes (NLs) to be delivered noninvasively to potentially treat and prevent the onset of AMD. The 220 nm NLs were composed of phosphatidylcholine and cholesterol through vacuum evaporation, rehydration, and extrusion. Our curcumin-loaded NLs were assessed using an *in vitro* oxidative stress model of ARPE-19 cells. MTT cell viability assay results show that the liposomal curcumin complex has been able to improve cell viability with respect to the untreated cells (28% more viable, $p < 0.05$),

and cells that were damaged with peroxide (50% more viable, $p < 0.05$). As a preventative measure, the liposomal curcumin complex has been able to improve cell viability with respect to untreated cells (55% more viable, $p < 0.05$). *Ex vivo* modeling tested the permeability of the nanoliposomes to the posterior hemisphere of a porcine eye with a Franz diffusion cell apparatus. Qualitative fluorescence analysis shows that the nanoliposomes were able to permeate through different layers of the eye and reach the retina. *In vitro* studies with RPE cells show the treatment significantly reduces oxidative stress in cells while increasing cell viability, thus indicating that curcumin has potential to both treat and prevent AMD.

EVALUATION OF CURCUMIN-LOADED NANOLIPOSOMES FOR THE TREATMENT AND PREVENTION OF AGE-RELATED MACULAR DEGENERATION

By

Sriramya Ayyagari, Haris Dar, Vivian Morton, Kevin Moy, Chadni Patel, Lalithasri Ramasubramanian, Nivetita Ravi, Samantha Wood, Andrew Zhao, Melanie Zheng, Kiet Zhou

Thesis submitted in partial fulfillment of the requirements of the Gemstone Program
University of Maryland, 2017

Advisory Committee:

Dr. Justin Kerr
Dr. Michaela Mathews
Dr. Silvia Muro
Dr. Zhihong Nie
Dr. Nam Sun Wang

ACKNOWLEDGEMENTS

Team INJECT would like to thank all those who have helped us over the years. First and foremost, we would like to thank Dr. Helim Aranda-Espinoza for his invaluable guidance, time, and resources along every step of our research. We would like to thank Dr. Katrina Adlerz and the Cell Biophysics lab group for their guidance. To the Gemstone staff, thank you for your support and encouragement, and for this truly unique opportunity and experience. To Dr. Justin Kerr, thank you for your expertise and helping hand. To Ms. Yan Guo, thank you for your laboratory training. To Dr. Giuliano Scarcelli and his lab group, thank you for your help with our *ex vivo* studies. Thank you to our LaunchUMD donors and the University of Maryland Libraries for making our research possible. Without any of these people or our friends and family, we would not be where we are today.

TABLE OF CONTENTS

INTRODUCTION

Age-related Macular Degeneration

Age-related macular degeneration (AMD) is one of the leading causes of vision loss in people over the age of 50. One of the primary theories for its pathophysiology pertains to harmful oxidative stresses in the retina (Lim, Mitchell, Seddon, Holz, & Wong, 2012). The onset of AMD occurs as a result of different environmental and physiological factors such as old age, obesity, tobacco use, and genes involved in significant signaling pathways (Lim et al., 2012). AMD damages the macula, the central region of the retina, which is mostly composed of millions of photoreceptor cells, causing the center of the field of vision to appear blurry or dark (National Eye Institute, 2013). This causes detrimental effects for the patients, as vision in the focal parts of their eyes is severely limited.

There are generally two classifications to the disease, dry and wet AMD. The less severe, but more prevalent version of AMD is dry AMD (Lim et al., 2012). Dry AMD is characterized by yellow deposits called drusen that form under the macula. Over time, build-up of these drusen on the macula causes atrophy of retinal pigment epithelium (RPE) cells, ultimately leading to photoreceptor cell death and loss of central vision (Binder, Stanzel, Krebs, & Glittenberg, 2007). The other form of the disease is neovascular AMD, also referred to as wet AMD (Lim et al., 2012). Wet AMD is caused by abnormal blood vessel growth due to the malfunctioning of the signaling protein, vascular endothelial growth factor (VEGF). This results in the angiogenesis of fragile new blood vessels that are prone to leakage of fluids and lipids into the retina, thus causing irreversible damage to the macula (Lim et al., 2012). However, only about ten

percent of patients who are diagnosed with dry AMD are also diagnosed with the wet type (National Eye Institute, 2013). Thus, prevention and treatment of dry AMD is a significant focus of current research.

Projections have shown that the number of people diagnosed with AMD will be around 196 million in 2020, and will increase to 288 million in 2040 (Wong, Su, Li, Cheung, Klein, Cheng, & Wong, 2014). The increase in diagnoses is especially relevant as researchers have predicted that more than two-thirds of affected patients, mostly in Asia, Africa, and Latin America will not have access to expensive or invasive therapies (Wong et al., 2014). Therefore, it has become of vital importance to develop an effective treatment that can effectively prevent and treat AMD while still being affordable and easy to self-administer.

Curcumin

Curcumin, the biologically active component of turmeric, is used in traditional medicine for centuries. In Southeast Asia, turmeric has been used as an antiseptic for cuts and burns, and in other parts of Asia, it has been used to treat diseases associated with abdominal pain (Prasad & Aggarwal, 2011). Its antioxidant, anti-inflammatory, and antiproliferative properties make it a useful treatment for a variety of illnesses including retinal diseases such as AMD (Bhawana, Basniwal, Buttar, Jain, & Jain, 2011). Curcumin is thought to be successful in protecting RPE cells from oxidative stress, thus helping to prevent the onset of AMD (Woo, Shin, Lee, Joe, Zheng, Yim, Callaway, & Chung, 2012). However, the integration of curcumin in the treatment of AMD according to modern medicine is difficult due to its hydrophobicity and subsequent low bioavailability

(Pescosolido, Giannotti, Plateroti, Pascarella, & Nebbioso, 2014). As a result, curcumin is not yet an accepted method for the treatment and prevention of AMD.

Justification for Research

Though a variety of treatments exist to halt the progression of AMD, there is no cure to regain the loss in vision. Additionally, current FDA approved treatments are available for the wet form of AMD and there are no commonly accepted treatments available for dry AMD. The treatments for wet AMD involve monthly intravitreal injections that deliver anti-VEGF drugs to the retina. These intravitreal injections to the eye prove to be both invasive and time consuming for patients. One major focus in present AMD research is improving intravitreal treatments and to reduce the frequency of injections by combining the anti-VEGF drugs with photodynamic therapy and corticosteroids.

A topical application through the form of eye drops would allow for ease of delivery of the drugs into the back of the eye. Additional research has also shown the benefits of utilizing nanoparticles as drug carriers for eye disease treatments. Studies have shown that nanoliposomes (NLs), nanoparticle vesicles formed from phospholipid bilayers, applied via eye drops, may be effective drug carriers to the posterior segment of the eye (Hironaka et al., 2011). These studies introduce the possibility of using liposomal nanoparticles contained in eye drops to develop a topical treatment for AMD.

We hypothesized that encapsulating curcumin within NLs would create a feasible and effective method of delivering curcumin to the retina. By manipulating a topical delivery system, we could lay the foundation for the development of a potential topical

treatment option for AMD. There is research regarding preventative measures for AMD, however, none have proven to be effective thus far. As a result, AMD treatment and prevention is a vital and necessary area of research that is of great interest to people concerned for their vision.

Research Questions and Hypotheses

The global aim of our research was to find a novel therapeutic compound to treat and prevent the progression of AMD by improving the bioavailability of curcumin through liposomal nanoparticle encapsulation to allow delivery to the RPE. We created curcumin-loaded NLs and tested them on ARPE-19 cell lines and excised eyes in order to answer the respective questions: (1) Can the curcumin-loaded NLs reduce oxidative stress levels in RPE cells without causing any cytotoxic effects? (2) Can the curcumin-loaded NLs be incorporated in a topical delivery system that can effectively reach the target RPE cells?

We hypothesize that the curcumin-loaded NLs would be successful in increasing the bioavailability of curcumin and thus reduce the oxidative stress levels in ARPE-19 cells. Furthermore, we expect to see that the complex would be effective as a topical delivery system and would be able to travel through the layers of the eye without causing damage to surrounding tissues.

LITERATURE REVIEW

The basis of our treatment model stems from the use of curcumin, a component of turmeric, with antioxidant properties. Our approach to intraocular delivery of this hydrophobic compound was the use of a nanoparticle for noninvasive, topical application.. To select the most suitable material to encapsulate curcumin, we surveyed a selection of available nanoparticles for their chemical properties and physiological effects. We also surveyed standard protocols for synthesizing and characterizing drug-loaded NLs, as well as methods for testing the treatment potential of a curcumin-loaded NL.

Age-related Macular Degeneration

AMD targets the macula, a small pigmented section of the retina. This area is composed of millions of photoreceptor cells, primarily the color-sensitive cone cells, and hence damage to this region causes the center of a person's field of vision to appear blurry and dark (National Eye Institute, 2013). In particular, despite the small size of the affected region, the high concentration of photoreceptors means that central visual acuity is approximately ten times stronger than that of the periphery. This central vision loss thus accounts for a major loss of one's sight. AMD is commonly divided into two forms: the less acute, but more prevalent "dry" AMD and the rapidly progressive neovascular, or "wet" AMD. Dry AMD is characterized by drusen, yellow deposits, forming underneath the macula. Many proteins and lipids have been found in drusen including apolipoprotein E (ApoE) and α, β-crystallin (Binder et al., 2007). Over time, the buildup of these deposits causes the RPE and photoreceptor atrophy. Dry AMD is classified into 3 stages:

early, intermediate, and late AMD. These stages are characterized by changes in the amount and size of drusen deposits, as well as the progression of RPE abnormalities. RPE abnormalities and vision loss are not seen until the intermediate stage. Data suggests that the progression between intermediate and late AMD typically occurs within 6.5 years. Symptoms during these stages include gradual vision deterioration, trouble adapting to changes in lighting, difficulty reading, and face recognition problems (National Academy of Sciences, 2015).

Neovascular, "wet" AMD (Lim et al., 2012) can either develop on its own or as a progression of dry AMD. Wet AMD is caused by abnormal blood vessel growth under the retina, stimulated by VEGF, a signal protein for angiogenesis and vasculogenesis. These new vessels are fragile and prone to leaking and spontaneous hemorrhage. Scarring from these broken blood vessels causes irreversible damage to the macula. Approximately only ten percent of patients who are diagnosed with AMD suffer from the wet type; however, they experience more severe vision loss (National Eye Institute, 2013).

AMD is a multifactorial disease. As its name implies, the most significant risk factor for AMD is old age, as the likelihood of developing AMD increases substantially as a person grows older (National Eye Institute, 2013). Recognized risk factors include cigarette smoking, Caucasian race, and positive family history. Other presumed risk factors include sunlight exposure, hyperlipidemia, hypertension, and vitamin deficiency. Various genes may play significant roles in the biological pathways related to the onset of AMD. For example, the VEGF-A gene is responsible for encoding the VEGF signaling protein, hence a mutation in this gene may lead to wet AMD (Lim et al., 2012).

Pathology. The pathogenesis of AMD is characterized by the degeneration of retinal photoreceptors, RPE, and Bruch's membrane (Ding, Patel & Chan, 2008). Little is known about the precise mechanisms that lead to the disease due to the complex interactions of inflammation, apoptosis, cholesterol trafficking, angiogenesis, and oxidative stress, all of which play a role in AMD progression (Ding, Patel & Chan, 2008). However, oxidative stress is known to play a central role in AMD pathogenesis. Studies have shown that those with AMD have higher levels of carbohydrates and lipids that have been modified by oxidation (Howes et al., 2004). However, the mechanism through which this oxidation occurs is not well understood. It is known that oxidative stress occurs when the cell is exposed to reactive oxygen species, whose sources can be both exogenous and endogenous (Kohen & Nyska, 2002). These reactive oxygen species then generate toxic hydroxyl radicals and hydrogen peroxide, which damage the cell through reactions with proteins, DNA, and lipids and eventually induce cell death (Ding, Patel & Chan, 2008). The exact reaction between the toxic radicals/hydrogen peroxide and cell components is not well defined.

AMD is asymptomatic in its early stages. It can be clinically diagnosed by finding drusen underneath the RPE, which appear as yellow spots in the macula. Although drusen accumulation is used to diagnose AMD, the mechanism through which it accumulates and its role in AMD pathogenesis and progression is unknown (Ding, Patel & Chan, 2008). Patients with dry AMD lose vision gradually over the years, while those who develop wet AMD experience rapid vision loss. Central vision is blurry, and straight lines seem distorted, which is referred to as metamorphopsia (Lim et al., 2012). As photoreceptor damage progresses, dark spots are seen in the center of their field of vision,

which is referred to as scotoma (Lim et al., 2012). In the advanced stage of AMD, patients completely lose central vision.

The RPE layer of eye tissue lies between the choroidal and neural tissues. The epithelial cells in this layer contain melanin, which aids in ensuring visual acuity by preventing light scattering. Additionally, the melanin granules absorb free radicals in order to protect the photoreceptors in the retina (Porte, 2012). However, melanin levels decrease with age, which leaves the retina vulnerable to the toxic effects of oxidative species. The toxicity leads to photoreceptor degradation (Curcio, Medeiros, and Millican, 1996). Additionally, RPE cells are important in removing waste products from photoreceptor degradation. Once they are degraded, the outer rod and cone segments are absorbed by the RPE cell cytoplasm and are formed into lipofuscin granules by the lysosomes. These granules are then released into the bloodstream as metabolic wastes. However, levels of lipofuscin increase with age due to decrease melanin and overall antioxidant activity that lead to photoreceptor toxicity (Porte, 2012). The accumulation of lipofuscin granules, along with other waste products, leads to the build-up of drusen that characterizes dry AMD.

Treatment. Although there is currently no definitive cure for AMD, recently, a variety of treatments have been developed for the wet form of AMD. Among the most effective treatments are anti-VEGF drugs, which combat abnormal angiogenesis. Ranibizumab, for example, is currently the most efficient in treating AMD. Clinical studies have shown that Ranibizumab prevented vision loss in 95% of patients and significantly improved vision in 40% (Rosenfeld et al., 2006). Bevacizumab is another successful anti-VEGF drug. Its efficacy is similar to that of Ranibizumab but is much less expensive and

therefore a more popular choice of treatment (Gerson, 2009). Other effective anti-VEGF drugs include Aflibercept and Pegaptanib (Lim et al., 2012). However, despite the effectiveness of the anti-VEGF drugs, they have several drawbacks. Drugs like Ranibizumab and Bevacizumab require a strict regimen of monthly intravitreal injections, which are not only inconvenient, but also invasive with potential health risks (Lim et al., 2012). Systemic side effects of these drugs include higher risks of strokes, myocardial infarctions, and other vascular complications (Lim et al., 2012).

Several other experimental treatments with varying effectiveness are available. One such treatment is an RPE transplant (Binder et al., 2007). Pilot studies have shown that 57% of patients who underwent RPE transplantation saw their visual acuity improve, while 7% of patients had their acuity decrease. However, Binder et al. (2007) found several limitations. They could only use autologous RPE transplants, as allogeneic RPE transplants often induced adverse immune responses. The constraints of autologous transplants limited the graft size that was available for transplant and were not helpful in offsetting any genetic factors associated with the onset of AMD. Autologous transplants can also induce damage on the transplanted tissue during the surgery. Furthermore, RPE transplants have much higher safety risks than that of the anti-VEGF treatments, making them less than ideal for common AMD treatment, especially considering the prevalence of the disease. Another alternative is the implantation of synthetic telescope lenses, which is approved by the FDA to treat late stage AMD (Hudson et al. 2008). This telescope replaces the eye's natural lens and essentially magnifies the field of vision while limiting peripheral vision. While effective, this surgery is invasive and comes with a set of risks, including damage to other parts of the eye (e.g. corneal edema), difficulty with

rehabilitation post-surgery, and other surgical complications.

Prevention. Despite the recently developed treatments, prevention of AMD is of great importance, since AMD cannot be cured or reversed in its advanced stages. Most preventative measures include lifestyle changes to reduce the risk factors for AMD. Studies have confirmed that there is a positive correlation between smoking, excessive sunlight exposure, cardiovascular disease, and lack of proper diet and exercise to the onset of AMD (Snodderly, 1995). Eliminating preventable risk factors would help decrease the chances of developing AMD. Researchers have found that carotenoids and antioxidants play extremely vital roles in preventing AMD as they help protect the retina from oxidative stresses. Two carotenoids, lutein and zeaxanthin, have been found to be very important as macular pigments that specifically safeguard the macula from the destructive oxidative processes in the retina (Snodderly, 1995). The intake of these carotenoids as part of the diet has been found to be most beneficial, though the same does not hold true for blood carotenoids. Similarly, vitamins E and C have been found to demonstrate significant protective measures. High-dose antioxidants and minerals (mostly zinc) were found to delay progression of AMD from the early-intermediate stages to advanced stage (Age-Related Eye Disease Study Research Group, 2001). However, vitamin and antioxidant supplements are not completely effective in treating AMD or slowing its progression in its later stages.

Current Research. AMD research efforts focus more on the treatment of AMD than its prevention, and in particular wet rather than dry AMD. One focus area has been improving anti-VEGF treatments by combining the anti-VEGF drugs with photodynamic therapy and corticosteroids (Spaide, Sorenson, & Maranan, 2003). These treatments

combine the immediate and distinct improvements from photodynamic therapy with the longer lasting benefits of anti-VEGF drug therapy. Corticosteroids supplement the therapy with antiangiogenic and anti-inflammatory effects. But even this combination of therapy is often not effective.

Current research is also looking towards the use of stem cell therapy to regenerate damaged retinal cells. Embryonic stem cells can be used to help replenish the loss of photoreceptor cells within the eye in patients with advanced AMD (Lim et al., 2012). Within AMD prevention research, one of the main focuses is improving screening and detection methods for AMD. Recent studies have reported progress in detecting AMD symptoms and markers from retinal photographs with a sensitivity and specificity rate of 75% (Quellec, Russell, & Abramoff, 2011). Nevertheless, research on the prevention of AMD is still considerably limited. Further research could potentially help lessen the destructive effects of AMD by diagnosing the disease at an earlier stage.

Topical Application

Anatomy of the Eye. The anatomy of the eye is a significant barrier to treating AMD due to the location and physiologic properties of the retina where the oxidative damage occurs.

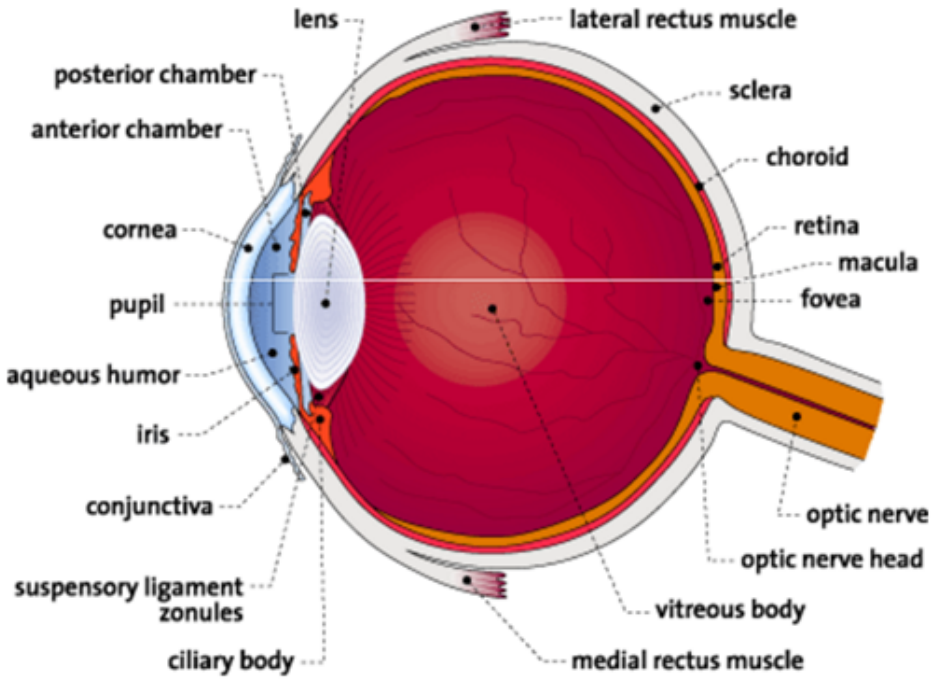

Figure 1. Human eye anatomy, parts of the eye explained (Bagi, n.d.).

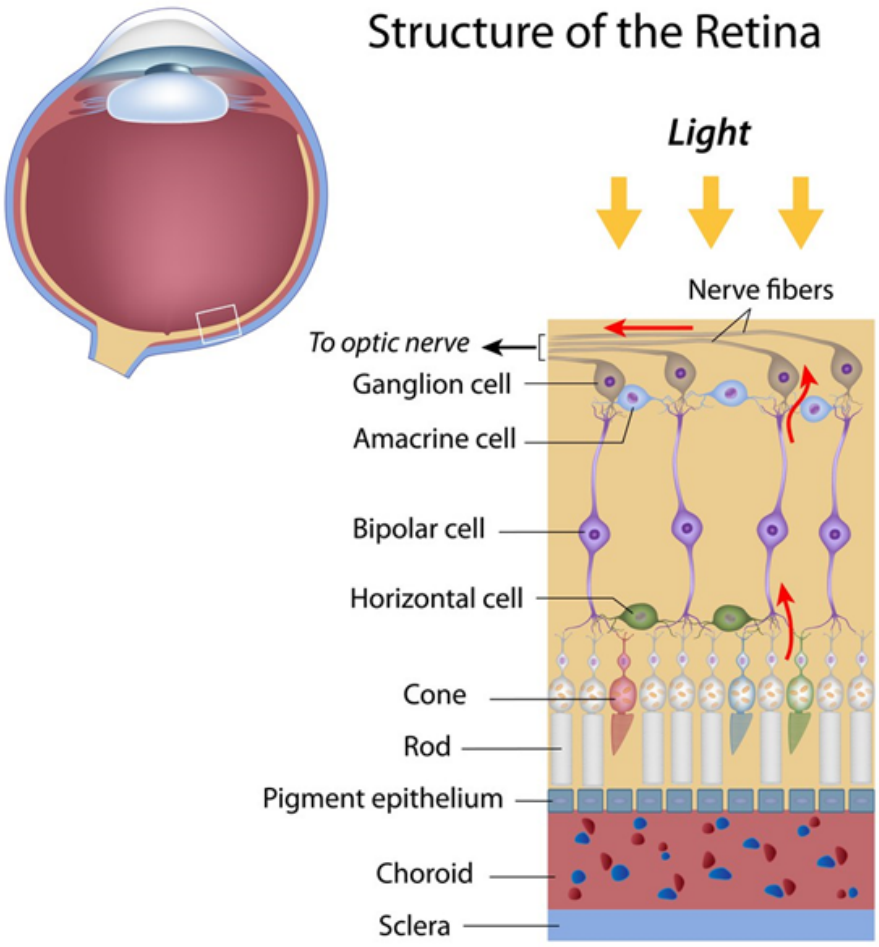

Figure 2. Structure of the retina (© Alila Medical Media, standard license)

Ocular-brain barriers act to selectively permit molecules into and out of the eye. In the front of the eye, the blood-aqueous barrier (BAB) is most relevant in cases involving the cornea and the lens. The blood-retinal barrier (BRB) governs the interaction between the retina and blood. The BRB is made up of two areas: one interacting with retinal vessels and one interacting with the choroid-RPE surface. These blood-ocular barriers are similar in that the inner BRB does not diffuse molecules larger than 20-30 kDa, while the outer layer tends to support diffusion of about the same nature, carrying in glucose and electrolytes (Chen, Hou, Tai, & Lin, 2008).

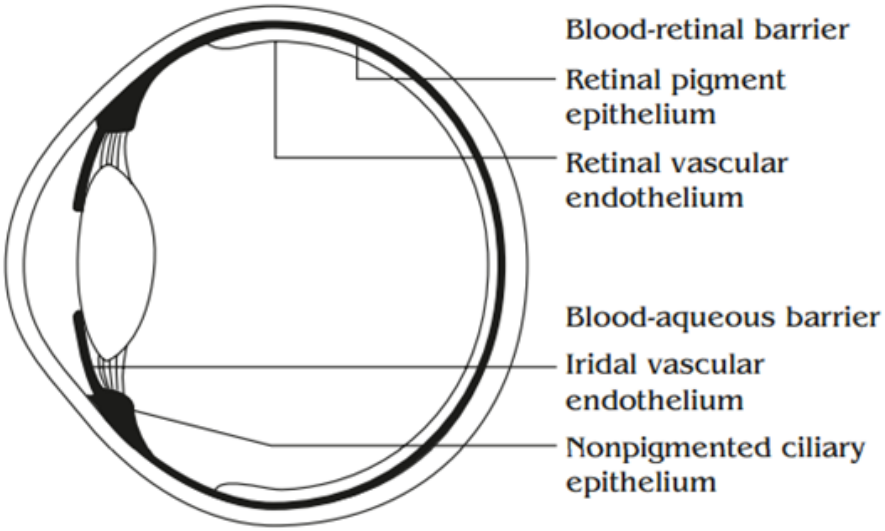

Figure 3. Location of ocular-brain barriers (Chen et al., 2008).

Targeting the Posterior Eye. Permeability of a topical drug targeting the posterior region of the eye is a key factor in overcoming ocular barriers. Success depends on reaching the target cells while maintaining effective treatment capabilities.

One study showed that a solution of the potential AMD treatment drug P2X antagonist pyridoxalphosphate-6-azophenyl-2',4'-disulphonicacid (PPADS), successfully reached the back of the eye. The drug specifically protected the cells against cell lysis, indicating close interaction with the cells (Birke, Lipo, Birke, & Kumar-Singh, 2013). This treatment has relevance to our study by showing that topical application has the capacity to reach the target cells of interest in AMD.

Encapsulation may be necessary for *in vivo* AMD therapy to increase the bioavailability of a drug. In this case, liposomes are an effective tool to reach the retinal cells of the eye. Of the surface modifiers tested, chitosan modification increased the efficacy of the drug the most (Sasaki et al., 2013).

Crossing Barriers in the Eye. The mechanical challenge in reaching the back of the eye

is crossing the various biological barriers of the eye. Choonara (2010) found that the ocular-blood barriers keep eye drops from being an effective treatment of posterior eye segment diseases. In an effort to develop a topical application of Avastin to treat AMD, Davis et al, (2014) used liposomes to encapsulate Annexin-5, a component of Avastin, to topically deliver to retinal cells within the rat eye. Liposomes successfully crossed the corneal epithelial barriers in order to reach the posterior of the eye (Davis et al., 2014). Modification of the liposome is also an important aspect of drug delivery. Sasaki et al. (2013) presented the potential to test the physicochemical properties of surface-modified liposomes *in vitro*, with success in application of the physicochemical properties when delivering drugs *in vivo*. The study specifically cites poly-L-lysine to modify the surfaces of the liposome (Sasaki et al., 2013). These case studies provide evidence that the use specifically of liposomal encapsulation makes reaching the back of the eye possible, and that surface modification may play a role.

Improving Topical Applications. There are two main issues with topical drug delivery to the eye: penetration through the cornea and penetration through the blood-brain barrier. This results in low drug absorption. In a 2002 study, researchers found that the addition of cyclodextrins to the eye drop solution greatly enhanced the absorption of the drug (Loftsson & Stefánsson, 2002). It also increased the water solubility and stability of the drug. Another study ran into a similar problem of low drug absorption (in particular, delivering insulin via eye drops) (Xuan, McClellan, Moore, & Chiou, 2005). Modifications, such as an increase in pH to 8.0 and the addition of absorption enhancers like glycocholate and fusidic acid, allowed for greater insulin absorption. Another study investigating drug delivery to the back of the eye using lipid-based eye drops found that

surface-modified lipid emulsions could be used as a way to deliver the hydrophobic drugs to the ocular posterior segment of the eye (Ying, Tahara, & Takeuchi, 2013).

Testing of Topical Application. *Ex vivo* studies have been used in order to evaluate the efficiency of eye drops in various animal models. Many of these studies have focused on targeting the cornea, in the anterior of the eye, though there are some that have demonstrated the potential for retinal drug delivery. For instance, bovine eyes were excised and used in order to determine how effectively luteinizing hormone-releasing hormone (LHRH) permeates the cornea and the other parts of the eye. The study found that the hormone localized to parts of the ocular endothelium, but not the vitreous. Evaluation of topical treatments to the back of the eye has been challenging, as the RPE is highly selective. However, a study by Kansara and Mitra (2006) demonstrated that mannitol could diffuse to the retina via the sclera and that permeability did not differ significantly between the sclera → retina pathway and the retina → sclera pathway.

Curcumin

Physiochemical Properties. Within the last decade, many scientists and researchers have discovered the therapeutic benefits of curcumin, an extract from the Indian spice turmeric with chemical formula $C_{21}H_{20}O_6$ (see Appendix B for the complete structure) and molecular weight 368.38 g/mol. Although curcumin has been commonly used in traditional and holistic medicine therapies, its use in clinical medicine has been limited due to its low solubility (< 0.1 mM in water) and its resulting poor bioavailability (Yadav, Suresh, Devi, & Yadav, 2009). However, multiple studies have found that curcumin possesses anti-inflammatory and antioxidant properties. Beloqui et al. found

that curcumin-loaded lipid-based nanocarriers reduced MPO and TNF-α enzyme activity *in vivo*, both indicators of inflammatory responses brought on by colitis (Beloqui et al., 2016. Kant et al. found that the antioxidant and anti-inflammatory properties of curcumin accelerated the cutaneous wound healing of diabetic rats. Curcumin was found to decrease the expressions of inflammatory enzymes and increased wound contraction (Kant et al., 2014). These long studied anti-inflammatory and antioxidant properties have more recently been studied across many diseases characterized by inflammation and oxidation. The goal of many of these studies is to increase the bioavailability and retention of curcumin in the body to improve efficacy of these treatments.

Curcumin is a free radical scavenger and can regulate cellular signal transduction pathways, which makes it potentially useful in treating cancer, neurodegenerative disorders, and diabetes (Calabrese et. al., 2008). Curcumin's capability to regulate mitochondrial processes and ATP production gives it a rare potential to treat and possibly prevent oxidative stress (Molina-Jijón et al., 2011). In addition, curcumin can down-regulate transcription factor NF-kB and NF-kB-regulated gene products, which have been linked to the onset of several chronic inflammatory diseases (Mandal et al., 2009). These properties of curcumin make it a candidate for treating the oxidative damage and inflammation related to AMD.

Retinoprotective Properties. Curcumin's ability to act as a retinoprotective agent has been shown in models of diseases induced by oxidative stress to the retina, including AMD (Fiorentino, Prioletta, Zuo, & Folli, 2013; Salem, Abdel-Rahman, Ewias, & Tsegay, 2012; Woo et al., 2012). Curcumin has been able to reduce the oxidative stress in RPE cells by increasing the production of hemeoxygenase-1 (HO-1) and decreasing

reactive oxygen species (ROS) production (Fiorentino et al., 2013; Woo et al., 2012). ROS pathways have also been shown as a possible mechanism for the development of AMD (Woo et al., 2012). Aside from RPE cells, curcumin has been shown to protect other cells in the eye.. For instance, curcumin has been shown to protect the cornea against nicotine-induced toxicity, which is an important risk factor for eye-related disease (Karam, Issa, Mohamed, & Hassanin, 2014). However, curcumin's ability to reverse pre-existing AMD damage has not been established.

Improvement of Visual Acuity. Mirza et al. (2013) found that curcumin and docosahexaenoic acid (DHA) worked well together and that the mice given both as a dietary supplement had significantly higher visual acuity compared to that of the control mice, while weakening the progression of retinal degradation. Mazzolani (2012) studied the lipid-based encapsulation of curcumin and found that it was effective in improving visual acuity for patients suffering from central serous chorioretinopathy.

Cytotoxicity Limitations. Despite the benefits of curcumin as a potential drug for treatment of AMD, there are some cytotoxicity concerns to consider. Several studies have demonstrated that greater than 20 μM doses of curcumin in the eye do not show therapeutic effects (Hollborn et al., 2013), and prolonged exposure affected caspase-3 activation, which can lead to necrosis and delayed apoptosis. These mechanisms are still being investigated. The bioavailability of curcumin has been shown to peak around 15 μM, where expression of HO-1 was highest (Hollborn et al., 2013). Although high concentrations of curcumin cause cell damage and death, a lower, controlled dosage still has potential to prevent the progression of AMD and other diseases involving oxidative stress. With the cytotoxicity of curcumin in mind, the conditions of cytotoxicity may

change given encapsulation of the drug. MTT assays may be used to evaluate this cytotoxicity when incorporated into a complex.

For molecules whose biodegradable properties are not as well known, Anitha et al. (2011) used an MTT assay to measure the cytotoxicity of carboxymethyl chitosan (*O*-CMC)-curcumin complexes. They measured cell uptake through cell culture studies and tracked curcumin molecules under a fluorescence microscope. This method also confirmed whether or not curcumin was actually released by the chitosan carrier. The study found that this chitosan derivative alone is not cytotoxic, while curcumin and the *O*-CMC-curcumin complex are cytotoxic only to cancer cells. The cell uptake results also showed a considerable increase in uptake of the curcumin when encapsulated by *O*-CMC, compared to that of free curcumin.

Clinical Targets. Several clinical trials have attempted to improve the biosolubility of curcumin by encapsulating it in a carrier. For instance, Marczylo et al. and Allegri et al. studied Norflo tablets in clinical trials to treat uveitis, which, like AMD, is characterized by inflammation in the eye . They used a phosphatidylcholine-based vesicle, to orally deliver curcumin. This was shown to significantly improve curcumin's bioavailability and tolerability (Marczylo et al., 2007; Allegri, Mastromarino, & Neri, 2010). Another study conducted by Shaikh, Ankola, Beniwal, Singh, & Kumar (2009) showed that PLGA (poly(lactic-co-glycolic acid)) nanoparticles improved oral bioavailability 9-fold and allowed a sustained release of curcumin for a period of 48 hours. One way in which encapsulation improves bioavailability is by increasing curcumin's half-life. A study done by Anand, Kunnumakkara, Newman, and Aggarwal in 2007 found the half-life of curcumin to be 0.31+/-0.07 hours. However, this half-life was 1.5 times longer when

curcumin was encapsulated in liposomes (Anand, Kunnumakkara, Newman, and Aggarwal, 2007). Their results demonstrate the successes in using nanoparticle encapsulation to overcome the limitations that come with using curcumin.

Nanoparticles

The use of nanoparticle technology has greatly increased in medicine, and especially in the field of retinal drug delivery. Nanoparticles range in size from 1 to 100 nanometers in diameter. They act as whole units in terms of transport and physical characterization and offer favorable properties of both bulk materials and molecular structures. The increased surface-area-to-volume ratio in nanoparticles also provides various opportunities for modification (Taylor et al., 2013). Nanoparticle drug delivery systems have particular potential in treating dry AMD in the posterior segment of the eye due to their capabilities in defying ocular barriers, targeting retina, and enhancing permeation, all while providing a controlled release (Kaur & Kakkar, 2014). However, there is also a delicate balance between a nanoparticle's capabilities and limitations that must be considered. In selecting the best-suited carrier for curcumin-encapsulating nanoparticles, we considered factors such as toxicity, size, biodegradability, stability, and feasibility of synthesis.

Magnetic Nanoparticles. Magnetic nanoparticles are becoming increasingly popular in ocular applications. Due to their surface properties and controlled manipulation for specificity, they have been utilized in various eye disease therapies. Their ability to be tracked by MRI also allows for a more controlled monitor of their movement and progression through the eye. A study by Giannaccini et al. (2014) showed that magnetic

nanoparticles that were intravenously injected localized in the RPE layer within 24 hours of delivery, suggesting their capabilities to challenge ocular barriers. The nanoparticles were retained within the ocular compartments for a longer period of time without disturbance from external influences. However, these properties have not yet been explored in mammalian organisms (Giannaccini et al., 2014). Furthermore, the lack of information that is attributed to these types of nanoparticles and their effects in encapsulation make it difficult to quantify their significance in drug delivery treatments.

Hydrogel Nanoparticles. Hydrogel nanoparticles have long been valued as a biocompatible drug delivery system due to their unique combination of hydrophilicity, high water content, and small size. These properties make them ideal for cellular drug delivery. Hydrogels are known for resembling living tissue cells more than any other type of synthetic biomaterial. However, the complexity of their release mechanisms also results in a complex balance in the development of these hydrogel nanoparticles, making them difficult to work with and to accurately produce (Hamidi, Azadi, & Rafiei, 2008).

Chitosan is a hydrogel that is a natural biopolymer produced by the fermentation of microorganisms (Rampino, Borgogna, Blasi, Bellich, & Cesàro, 2013). Chitosan, because of its natural composition, exhibits low cytotoxicity and soft tissue compatibility (Liu et al., 2013). Additionally, due to its precision time-release delivery, it can be used at both intra and extraocular levels (Agnihotri, Mallikarjuna, & Aminabhavi, 2004). It has been tested extensively as a nanoparticle that can encapsulate and deliver drugs for the treatment of many medical issues, from inflammation to cancer. Chitosan-curcumin complexes though, have been shown to demonstrate poor solubility, due to chitosan's hydrophilicity.

Polymeric Nanoparticles. Polymeric nanoparticles (PNPs) are made from various polymers and are also biodegradable, nontoxic, and nonimmunogenic. PNPs have been shown to non-toxically stay in cells for up to four months whilst continuously delivering drugs; this capability proves extremely beneficial in the long-term treatment of diseases. PNPs have been used extensively with curcumin to treat cancer. For instance, the study conducted by Bisht showed that encapsulating curcumin in PNPs successfully made the hydrophobic curcumin soluble in aqueous solution, allowing the body to uptake the curcumin and benefit from its antioxidant effects (2007). PNPs offer many advantages in controlled ocular drug release, as they can track the location of fluorescently labeled particles (Kaur & Kakkar, 2014). However, research also suggests that PNPs exhibit poor batch-to-batch reproducibility, which could prevent consistent experimentation and robust evaluation of the nanoparticle's therapeutic ability (Jawahar & Meyyanathan, 2012). While PNPs show much promise in the future, there is not enough current research to conclude that they have applications on the intraocular level.

Liposomes. Liposomes are amphiphilic compounds composed of a lipid bilayer and an aqueous compartment, allowing for full encapsulation of polar and nonpolar drugs (Kaur & Kakkar, 2014). Although liposomes may be difficult to load with drugs and have a relatively short shelf life, recent studies have shown that these limitations can be addressed through further manipulation of different variables (Meerovich et al., 2008). For example, the addition of polyethylene glycol (PEG) and surface proteins on these nanoparticles have allowed for improvements on long-circulating liposomes (Nguyen et al., 2008). Furthermore, liposomal targeting can easily be manipulated through the attachment of various antibody and protein fragments (Park et al., 2002). This class of

nanoparticles can also be utilized to target AMD and other retinal disorders. In a study conducted by Davis et al. (2014), Annexin A5-treated liposomes were utilized to deliver Avastin to the posterior region of the eye through a topical application. These nanoparticles were able to successfully cross the ocular barriers and deliver Avastin to the designated location, thus hinting at a sufficient transfer of liposomes into ocular compartments from an alternative route of delivery.

Lipid-based nanoparticles, or NLs, appear to be the appropriate carrier for a curcumin-laden nanoparticle to the posterior segment of the eye. This can be attributed to a combination of factors such as the low cost of production, amphiphilic nature, targeting capabilities, and previous success in similar endeavors. Potential setbacks, such as NLs' relatively short shelf life, can be improved by additional surface attachments. These aspects of lipid-based nanoparticles both for and against their use in topical applications have been carefully weighed to maximize the potential for success in delivering curcumin antioxidants to the RPE.

Lipid-based carriers are appropriate for cellular drug delivery because of the target's high lipid content. Nanostructured lipid carriers, when used to deliver the drug Zidovudine, exhibited high drug permeation in the body, and low toxicity (Gomes, Neves, & Sarmento, 2014). In addition, albumin, a matrix-forming macromolecule, was found to have high drug localization in the brain, high biodegradability and low toxicity. This highlights the lipid-based carriers' distinctive attributes, as the high biodegradability and low toxicity with high drug permeation makes them ideal for human drug delivery.

Drug-Membrane Interactions

The biophysical interactions of drugs such as curcumin with lipid membranes can be modeled by using a Langmuir model system. In this system, a well-defined and stable lipid monolayer can be formed on the surface of a liquid subphase using a Langmuir film balance. Using this monolayer, the interaction of drugs and drug delivery systems with lipids can be characterized through two different methods (Peetla, Stine, & Labhasetwar, 2009). One such technique involves compressing the lipid monolayer to a constant surface pressure. The drug or drug delivery system of interest is added to the subphase under constant film area and the subsequent changes in the surface pressure are recorded. The second method calls for a mixture of lipids and drugs to be spread on top of a subphase to form a monolayer. This monolayer is gradually compressed to create a surface pressure-film area isotherm, which is then compared with the isotherm of the pure lipid.

The Langmuir model can be used to determine the rate of drug penetration, maximum amount of drug penetrated and the saturation pressure of the membrane (Feng & Chien, 2003). Previous studies have extensively detailed the effects of drug penetration on the changes in surface pressure. One such study looked at paclitaxel, a chemotherapeutic drug, penetration into dipalmitoylphosphatidylcholine (DPPC) lipid membranes in order to model drug delivery to cervical cancer cells (Preetha, Huilgol, & Banerjee, 2006). Researchers specifically monitored the surface pressure changes. It was found that an increase in surface pressure with respect to time was due to the penetration of the drug while the eventual constant values with respect to time indicated the completion of drug penetration. The decrease of surface pressure with respect to time was

understood to be the result of the partial desorption of drug molecules from the monolayer while a negative surface pressure indicated the collapse of some of the monolayer into the subphase (Gicquaud, Chauvet, & Tancrède, 2003). Researchers have also investigated the effects of cholesterol on drug penetration. It was found that the addition of cholesterol to the DPPC lipid monolayer increased the membrane rigidity and significantly limited paclitaxel penetration (Zhao & Feng, 2006)

Additionally, the Langmuir trough has been used to investigate monolayer and, by extension, vesicle stability. As previously mentioned, a decrease in surface pressure after the addition of a drug indicates the desorption of lipid molecules into the subphase. This in turn suggests the destabilization effects of the drug at hand, as it disrupted the previously ordered structure to cause the some collapse into the subphase. One study specifically looked at the interactions of curcumin with monolayer and bilayer lipid membranes (Karewicz et al., 2011). Egg yolk phosphatidylcholine (EYPC) was used as the main component of the lipid membranes though cholesterol and dihexadecyl phosphate (DHP) were added to understand the effects of curcumin on the stability of mixed systems. As curcumin inserts itself preferentially into the liposomal bilayer, the vesicle characteristics are a direct result of the curcumin interactions with the lipid components of the vesicle. Karewicz et al. modeled these effects through a Langmuir monolayer model. They found that curcumin initially increases the particle size as its insertion into the membrane introduces stiffness to the layer. However, with increasing amounts of curcumin added, curcumin destabilizes the ordered lipid structure and decreases the particle size. Vesicle stability was also influenced by the addition of extra membrane constituents such as DHP and cholesterol. DHP was added to create

negatively charged liposomes that would have additional stability due to their polycationic coating. Isotherms of the EYPC/DHP and EYPC/DHP/Curcumin were similar, indicating that curcumin had similar interactions with the EYPC/DHP monolayer as it did with the pure EYPC monolayer. As such, the introduction of DHP to the monolayer was not effective in increasing the curcumin penetration. Cholesterol was included to the EYPC/DHP system to stabilize the liposomes as well as to limit drug leakage. Cholesterol was seen to insert itself into the bilayer in a method analogous to curcumin molecules. Cholesterol has a strong ordering influence on the monolayer structure, which counteracts the destabilization effect of curcumin. Cholesterol was found to be an advantageous addition to monolayer as it stabilized the overall liposome system proportionally to the curcumin loading content. EYPC/DHP, in contrast, destabilized quickly at drug loading. These results indicate that a mixed system of lipids and cholesterol is the most advantageous composition for effective drug loading and delivery.

Methodology Justification

We evaluated previously described methods for the synthesis of the curcumin-loaded NLs, *in vitro* testing, and *ex vivo* testing of the delivery system. This section aims to discuss procedures that were utilized for the project vision.

Curcumin-loaded Nanoliposome Synthesis Procedures. When synthesizing our curcumin-loaded NLs, we aimed to use a molecule susceptible to biodegradation so that it may be easily flushed out of the body. Some options included PLGA, which was tested by Grama et al. (2013) for its ability to improve the bioavailability of curcumin. In particular, they sought to treat diabetes-induced cataracts through ingestion of the

complex. PLGA was chosen for its well-known biodegradable and biocompatible properties. The loading of curcumin was done through stirring and suspension methods, followed by purification using an emulsion-diffusion-evaporation technique. The resulting pellet was then resuspended and freeze dried for storing in order to increase the drug's shelf life; characterization was carried out via dynamic light scattering at each major step and the study found no nanostructural discrepancies between the freshly-prepared stock and the freeze dried stock. Although the *in vivo* methods are outside the scope of this project, it should be noted that the results demonstrated a 9-fold increase in the peroral bioavailability of curcumin. These techniques can be combined with other lipids, to create a similar increase in bioavailability.

Studying liposomes as well, Puri et al. (2011) integrated fluorescent lipid probes into the synthesis procedure mixing in 0.5% mol lissamine rhodamine B before freeze-drying the lipids. They used fluorescence imaging to detect the conformation of different lipids in the bilayer.

Measuring Oxidative Stress. The retina is susceptible to oxidative stress on a daily basis due to its high oxygen consumption, great proportion of polyunsaturated fatty acids, and exposure to visible light (Totan et al., 2009). As mentioned previously, oxidative damage has a large role in the pathogenesis of AMD; therefore it is important to quantify oxidative stress when doing research on AMD.

Levels of reactive oxygen species (ROS) are important biomarkers to test. ROS are molecules that are produced as a result of aerobic metabolism and respiration and include hydrogen peroxide (H_2O_2), superoxide anion (O_2^-), and hydroxyl radicals (OH^-). Oxidative stress directly refers to increased levels of ROS, which can cause significant

damage to various biomolecules within the cells (Schieber & Chandel, 2014). By measuring ROS levels within the cells, it allows for another direct quantification of the oxidative stress that has been induced within. In addition to testing for ROS levels as a whole, it is also beneficial to look at biomarkers that target a specific component of ROS. Superoxide dismutases (SODs) are antioxidant enzymes that can convert a component of ROS, superoxide anion (O_2^-), to hydrogen peroxide (H_2O_2) and molecular oxygen. These are then further converted into water by other enzymes. This function allows SODs to serve as a principal defense system to protect biomolecules from oxidative stress and damage as these toxic molecules are converted to an innocuous product (Weydert & Cullen, 2010). The presence of significant amounts of SODs within a cellular environment indicate that concentrations of superoxide anion are kept low, and thus by measuring SOD levels, it allows for a quantification of the antioxidant activity in response to oxidative stress within the cells (Weydert & Cullen, 2010). The various biomarkers and steps offered for measuring oxidative stress should be taken before and after applying an experimental treatment in order to efficiently evaluate the effectiveness of the treatment.

Demonstrating Complex Permeation. A method to test complex permeation *ex vivo* is simulated posterior eye diffusion via a Franz diffusion cell. The tissues of interest are placed in the apparatus; with the drug solution placed in the donor chamber and simulated tear and vitreous fluids in the receptor chamber (Kaskoos, 2014). This process allows more control than submersion methods, as one can decide which tissues (i.e. which layers of the eye) are to be tested and where the localization of treatment occurs.

SUMMARY OF AIMS

Our research process was divided into three aims in order to better answer our overarching research questions. These aims include:

I. Creation of curcumin-loaded NLs in order to improve the bioavailability of curcumin.

II. Determination of the curcumin-loaded NLs' ability to allow significant release of curcumin into RPE cells and to reduce oxidative stress.

III. Demonstration of a topical delivery application for the curcumin-loaded NLs in order to establish its permeability through the eye.

In terms of the first aim, we hypothesized that if curcumin could be encapsulated in a liposome, the bioavailability of curcumin would increase. Additionally, the hydrophobic curcumin would remain in the lipid bilayer of the liposome allowing it to be delivered to target locations. In terms of the second aim, we hypothesized that RPE cells that are treated with the curcumin-loaded NLs would reduce oxidative stress. In terms of the third aim, we hypothesized that the curcumin-loaded NLs delivered to excised porcine eyes would permeate through the eye and reach the retinal layer.

METHODOLOGY

Aim I: Synthesis of the Curcumin-loaded Nanoliposomes

Preparation of Solutions

Cholesterol. Powdered cholesterol was purchased from Avanti Polar Lipids. A stock solution was created by dissolving 12.5 mg of cholesterol in 1 mL of chloroform.

Curcumin. To prepare the free curcumin solution, curcumin purchased from Sigma Aldrich (97% purity) was dissolved at 25 mg/mL in dimethyl sulfoxide (DMSO) and stored at 4°C to maintain stability. This stock solution was then diluted for all liposomal preparation, *in vitro* and *ex vivo* studies.

Preparation of the Curcumin-loaded Nanoliposomes. Curcumin-loaded NLs were prepared using the thin-film hydration method. Egg yolk phosphatidylcholine (Avanti Polar Lipids) and cholesterol solutions were both dissolved in chloroform and then mixed in a 4:1 molar ratio respectively. Curcumin was added in a 1:1 molar ratio with the total amount of lipids (phosphatidylcholine and cholesterol) into a glass vial. Though curcumin is naturally fluorescent in the visible green spectrum, a molecular probe, lissamine rhodamine B (Avanti Polar Lipids), was added at a molar ratio of 1:2000 of dye: phosphatidylcholine in order to fluorescently tag the phosphate heads of the phosphatidylcholine and allow for better visualization. The lissamine rhodamine B tag was fluorescent in the visible red spectrum.

Once the lipids were thoroughly mixed, the vial was rotated slowly to spread an even film along the sides of the container. The excess chloroform solvent was then removed by placing the vial in a vacuum chamber for three hours in order to obtain a dry lipid film. The lipid film was rehydrated with 0.270 M sucrose solution and agitated.

Upon rehydration of the film, the phospholipids self-assembled into vesicles featuring lipid bilayers; the aqueous solution is pushed toward the hydrophilic heads, while the hydrophobic tails host an environment favorable for the curcumin – inside the bilayer itself. Twelve hours after rehydration, the NLs were extruded through 200 nm polycarbonate membranes (Avanti Polar Lipids) using an extruder (Avanti Mini Extruder, Avanti Polar Lipids) to obtain a homogeneous solution of 200 nm diameter NLs.

Characterization of the Curcumin-loaded Nanoliposomes. Microscopy techniques were used to visualize the NLs for qualitative analysis. Nanoparticle tracking analysis (NTA) and ultraviolet-visible (UV-Vis) spectroscopy were used to determine size and encapsulation efficiency of the curcumin-loaded NLs respectively. Langmuir trough monolayer studies were also conducted to investigate the liposome membrane characteristics and the effect of curcumin on membrane stability.

Microscopy. The Olympus IX71 (Olympus Corporation) microscope was used to conduct standard fluorescent microscopy techniques that were used for the clear, quantifiable tracking of both the empty and curcumin-loaded NLs within cells and during *ex vivo* testing. As lissamine rhodamine B has an emission wavelength of 583 nm (Avanti Polar Lipids, 2017), all NLs were visualized using the FITC filter.

Nanoliposome size. Nanoparticle tracking analysis, through the Malvern NanoSight LM10 (Malvern Instruments), allows characterization of nanoparticles from 10 nM-2000 nM in the sucrose solution in which it is rehydrated. NTA uses direct observation and measurement of diffusion to analyze the nanoparticles. The NanoSight dually utilizes light scattering and Brownian motion of the particles in liquid suspension. Data collected

from this method include particle size distribution and statistics, concentration, and visual rendering of the curcumin-loaded NLs (Filipe, Hawe, & Jiskoot, 2010).

The curcumin-loaded NLs were prepared for the NanoSight LM10 by taking the rehydrated liposome solution, described prior in the methodology section, and diluting it 1:10000 in a 0.270 M sucrose solution in preparation for the imaging process. This created the clearest imaging for the NanoSight.

Encapsulation Efficiency. UV-Vis spectroscopy offers a clear, convenient procedure to quantify curcumin concentration within the curcumin-loaded NLs. The concentration of curcumin-loaded NLs was analyzed using a UV-spectrophotometer (NanoDrop 1000, Thermo Scientific) and a standard calibration curve.

The standard curve was made by initially dissolving free curcumin in DMSO to make a 0.6 M curcumin stock solution. A 1:3 serial dilution was used to dilute the curcumin stock solution in 0.270 M sucrose solution to make solutions with final curcumin concentrations between 1 nM and 2 mM. The concentrations in the samples were then quantitatively measured through UV-Vis spectroscopy, using the NanoDrop. The blank was sucrose when creating the standard calibration curve but for all subsequent experimentation where the concentration of curcumin in the curcumin-loaded NLs was being measured, the blank was empty NLs. Though literature showed that the excitation wavelength for curcumin is 424 nm (Kunwar et al., 2006), preliminary testing showed that the curcumin signals were stronger at 416 nm. Therefore, all subsequent UV-spectrophotometry experimentation were conducted at an excitation wavelength of 416 nm. Measurements were taken in triplicate to ensure accuracy in data. The average absorbance of the samples was plotted and Beer-Lambert Law was used to determine the

linear relationship between absorbance and concentration of curcumin in a sucrose solution.

$$\textit{Beer- Lambert Law}: A = a_\lambda \cdot b \cdot c$$

where A= absorbance, a_λ =wavelength-dependent absorptivity coefficient (found from the slope of the standard curve), b= path length (taken to be 1), and c= concentration.

The experimental NLs were similarly analyzed by taking multiple absorbance measurements at 416 nm. The concentrations of curcumin in the curcumin-loaded NLs were calculated by applying the linear relationship obtained from the standard curve.

The encapsulation efficiency of the NLs was quantified using the following equation:

$$Encapsulation\ efficiency\ (\%) = \frac{Loaded\ curcumin\ conc.}{Initial\ curcumin\ conc.} \times 100,$$

where loaded curcumin refers to the concentration of curcumin determined from UV-spectrophotometry data and Beer-Lambert Law calculations and initial curcumin refers to the concentration of curcumin added to the curcumin-loaded NL mixture (21.96 mM).

Drug Retention Studies. The shelf life of the curcumin-loaded liposomes was investigated by measuring the drug retention properties. Specifically, the amount of encapsulated curcumin was measured over time to determine the ability of the liposome retain the curcumin within its bilayer. Briefly, the nanoliposomes were fully synthesized on Day 1 and the absorbance readings were taken in triplicate periodically over a time interval of 15 days. The absorbance readings were converted into concentrations using Beer-Lambert Law (as described in the previous section) to calculate encapsulation

efficiency. The efficiencies were normalized with respect to Day 1 and subsequently plotted. A linear regression was applied to determine the correlation, if any, between time and encapsulation efficiency.

Langmuir Monolayer Studies. Langmuir monolayer experiments were performed on a Langmuir mini trough film balance (Kibron Microtrough XS, Kibron Inc., Finland).

Preparation. The trough was placed on a stable table and was enclosed by an environmental chamber. A 4-well multiwell Teflon microtrough plate **(**8x14 cm, 2.1 cm radius**)** was used for testing. Before each experiment, the trough was washed with ultrapure water and ethanol in sequence three times. The sensor probe was sterilized by passage through flame for approximately thirty seconds. The well was filled to the brim with ultrapure water, which served as the subphase for all subsequent experiments. The trough was calibrated with respect to the surface tension of the water subphase, which in this case was 72.8 mN/m. The probe was lowered into the subphase until it was approximately 2 centimeters below the surface. Before the start of each trial, the system was calibrated and zeroed. The accuracy of the system was found to be 0.001 mN/m.

Mixtures. Control mixtures of phosphatidylcholine (PC) and cholesterol (C) and experimental mixtures of phosphatidylcholine, cholesterol, and curcumin (Cur) were prepared at 4:1 PC:C, 1:1 PC:C, and pure PC molar ratios. See Appendix D for specific volumes. In all experimental conditions, the total lipid (PC and C) to curcumin molar ratio was kept constant at 1:1. The mixtures were diluted 1:50 in chloroform.

Testing. Each trial was begun by lowering the probe in water for 100 seconds to obtain a steady baseline measurement. A 10 μL Hamilton microsyringe (Hamilton Company) was used to carefully place a desired volume of a mixture on the surface of the subphase. The

lipid was expelled gradually in order to avoid membrane collapse and to create an even film on the water surface. The resulting surface tension was recorded with *Kibron FirmWare* until the system reached equilibrium.

Measurement. The recorded measurement was the ending surface tension value where the system reached equilibrium. The differences in equilibrium points between the pure lipid mix and the curcumin-lipid mix was compared to determine the effects of curcumin uptake by the lipid membranes.

Aim II: Testing the Nanoliposomes in Cell Culture

Experimental Conditions

Cell Culture Conditions. The curcumin-loaded NLs were assessed using an *in vitro* oxidative stress model. The Adult Retinal Pigment Epithelial 19 cell line (ARPE-19), purchased from ATCC, was selected in order to test the curcumin-loaded NLs, as this cell line was derived from the RPE cell layer in humans and is phenotypically similar to it. Cells were grown in Dulbecco's Modified Eagle Medium (DMEM, from Gibco) supplemented with 10% Fetal Bovine Serum (FBS, from ThermoFisher Scientific) and 1% PenStrep (ThermoFisher Scientific). Media was changed every two days, and cells were passaged at 90% confluency using 0.25% Trypsin-EDTA (ThermoFisher Scientific). Cell lines were maintained in a 37°C in a 5% CO_2 atmosphere.

Test Conditions. The curcumin-loaded NLs , free curcumin, empty NLs, and H_2O_2 experimental solutions were diluted using DMEM basal media, for all experiments.

Induction of Oxidative Stress. Oxidative stress was induced using H_2O_2. After washing cells two times with DMEM basal media, 30% weight/volume H_2O_2 purchased from

Sigma Aldrich was diluted in DMEM basal media to a final concentration of 600 μM. Cells were then incubated for 24 hours with this peroxide solution for all experimental procedures.

Curcumin-loaded NLs. The curcumin-loaded NLs were diluted in basal DMEM media to a final concentration of 10 μM curcumin. This was done by calculating the concentration of NLs, and assuming an encapsulation efficiency of 2-5%, based on the results from Aim 1. From this information, we were able to determine the volume required to give a final concentration of 10 μM curcumin in the loaded particles.

Empty NLs. The amount of empty NLs that was tested was calculated from the results of the curcumin-loaded NPs. From this information, we determined the total number of NLs that were tested. We then tested these many unloaded liposomes in this experimental sample.

Preparation of Fibronectin-Coated Glass Dishes. Glass dishes were coated with a Fibronectin solution (10 μL 100x Fibronectin + 90 μL 1X Phosphate Buffered Saline) and incubated at room temperature for 2 hours. Dishes were washed 3 times with 1X PBS, after which cells were plated.

Preventative and Treatment Models. We tested our curcumin-loaded NLs using two approaches: a preventative model and a treatment model. The preventative condition was utilized in order to test the efficacy of the curcumin-loaded NLs as a preemptive measure for AMD, and determine whether oxidative damage could be restricted or minimized. The treatment model was utilized in order to determine whether the curcumin-loaded NLs could be used to reverse or halt damage to cells that underwent oxidative stress. In both models, 30,000 cells/well were initially plated in a 96 well plate, and allowed to adhere

for 24 hours. All experiments were conducted in triplicate.

Preventative Model. In the preventative model, cells were washed with basal media 2 times before being treated with the following conditions: no treatment, free curcumin, empty NLs, curcumin-loaded NLs, H_2O_2, 4% DMSO, 100% DMSO for 24 hours prior to oxidative damage with H_2O_2. Cell viability and reactive oxidative species assays were then run at this point.

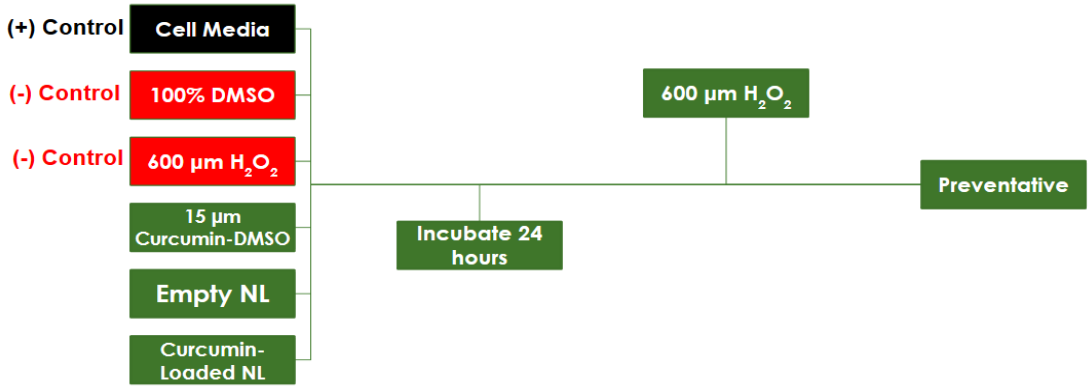

Figure 4. Preventative Model procedure flowchart

Treatment Model. For the treatment model, cells were initially damaged for 24 hours with H_2O_2 and incubated at 37°C in a 5% CO_2 atmosphere. Cells were then treated with the same seven experimental conditions (same as in the preventative model) and incubated for 24 hours. The cell viability and reactive oxidative species levels were then assayed.

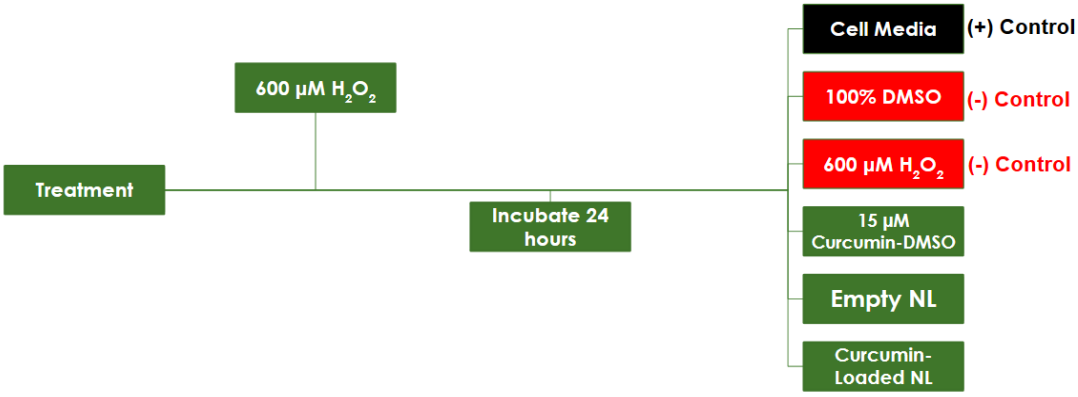

Figure 5. Treatment Model procedure flowchart

Time Lapse Studies with Fluorescence. In order to demonstrate the need for a curcumin-loaded NLs delivery system, time lapses of ARPE-19 cells were performed. 500,000 cells were incubated in 2 mL of 10 μM of curcumin-DMSO in basal DMEM. The suspension was thoroughly mixed to ensure that there was no aggregation of cells or curcumin and incubated in a test tube for 24 hours at 37°C. After overnight incubation, the suspension was centrifuged at 125g for 7 minutes. The remaining cell pellet was washed with 500 μL of 1X PBS and centrifuged at 125g for 7 minutes in order to remove the excess curcumin. Cells were then resuspended in 2 mL basal DMEM and plated on Fibronectin coated glass dishes, and allowed to adhere overnight. Cells were imaged using the Olympus IX71 microscope in brightfield at 10X. The curcumin was imaged at 424 nm. Fluorescence images and brightfield images were then overlaid in ImageJ to create a composite.

MTT Assay. The MTT (3-(4,5-dimethylthiazol-2-yl)-2,5-diphenyltetrazolium bromide) assay was used to evaluate the cytotoxicity and effect of the NLs on ARPE-19 cell proliferation. The assay utilized a colorimetric approach to assess metabolic activity of the cells as determined by the presence of a purple product. MTT would be uptaken by cells and reduced to formazan, which could then be detected colorimetrically. Thus, a higher amount of formazan would indicate higher metabolic activity and consequently more cells.

The MTT assay was performed according to the protocol from the MTT Cell Proliferation Assay Kit purchased from Cayman Chemical Company. 30,000 cells/well in 100 μL growth media were seeded onto a 96 well plate. All experimental conditions were conducted in triplicate. After both the preventative model and the treatment model were

created, 10 μL of the MTT reagent (provided in kit) was added to each well. Plates were gently mixed for one minute and incubated at 37°C for 4 hours. 100 μL of the Crystal Dissolving Solution (provided in kit) was added to each well and incubated for 18h at 37°C. Absorbance was read at 570 nm using a Microplate Reader (MolecularDevices SpectraMax). All data were normalized with respect to the untreated condition. For MTT reagent reconstitution, see Appendix J.

Reactive Oxygen Species Assay. The Reactive Oxygen Species (ROS) Assay was performed in order to assess the antioxidant activity of cells when treated with the curcumin-loaded NLs. In this assay, cells were pretreated with a 7'-Dichlorodihydrofluorescin diacetate (DCFH-DA), a cell-permeable non-fluorescent dye. Upon reaction with a reactive oxygen species, such as a free radical, DCFH-DA oxidizes to dichlorodihydrofluorescin (DCF), a fluorescent compound that could be quantitatively measured. A higher level of DCF would indicate more oxidative species and a lower level of DCF would indicate fewer oxygen species, suggesting that there was antioxidant activity. For the complete chemical reaction, see Appendix K.

ROS levels were determined through the procedures from the ROS Activity kit purchased from CellBioLabs. 30,000 cells were seeded in a 96 well plate and grown overnight. Cells were then washed once with basal DMEM, after which 100 μL DCFH-DA (1X, diluted in basal DMEM) was added. The plate was then incubated at 37 °C for 1 hour in the dark with the appropriate experimental conditions. The dye was then removed and plates were washed with 1X PBS, after which experimental conditions were added. After the preventative and treatment models were created, the ROS assay was conducted.

Media was first removed from each well. 100 μL of basal media and 100 μL of

the 2X cell lysis buffer was then added to each well, and mixed thoroughly to ensure cell lysis. Wells were then scraped to detach the cells completely. The plate was then incubated at room temperature for 5 minutes to allow lysis reaction to occur. 150 µL of the solution was transferred to another 96 well plate and read at 480 nm excitation and 530 nm emission using a microplate reader (MolecularDevices SpectraMax). ROS levels were quantified based on standard solutions (provided in kit) and extrapolating from the line of best fit.

Aim III: Drug Delivery Testing

The curcumin-loaded NLs topical solution was tested in an *ex vivo* eye model in order to demonstrate its efficacy and permeability. We proposed that curcumin-loaded NLs solution can (1) significantly permeate the layers of the eye and (2) localize in target tissues.

Eye Dissection. Fresh porcine eyes were obtained from Wagner's Meats (Mount Airy, MD, USA) in order to carry out permeability experimentations. Eyes were dissected by using dissection scissors to divide the anterior and posterior sections. The anterior portion of the eye and vitreous humor were then discarded and the posterior eye, comprised of the choroid and retina, was used for experimentation.

Franz Diffusion Chamber. Five mL of PBS was introduced into the Franz diffusion cell (see Appendix C) and the posterior eye was placed on the apparatus. After enclosing these layers in the capsule, 200 µL of the curcumin-loaded NL solution was placed on top of the tissue. The Franz cell was run for approximately 180 minutes to allow for complete NL diffusion through the tissue layers. Once the full cycle was run, the posterior portion

of the porcine eye was removed and washed with PBS in order to remove any fluid, including excess curcumin-loaded NL solution, that may have just been resting on the exterior of the eye. The *ex vivo* eye tissue was then imaged for the lissamine rhodamine B probes that marked the presence of the curcumin-loaded NLs. After initial examinations with the Franz cell running the full 180 minutes cycle, time-lapse studies were conducted in order to determine the influence of time on curcumin uptake. In these studies, the Franz cell run time were varied at 60, 135, and 210 minutes.

Statistical Analysis

Significance Testing

Size Distribution. A t-test on the size distribution and a F-test on the variations of these distributions was calculated, both at $\alpha = 0.05$. The size distributions were taken from the nanoparticle tracking analysis from the NanoSight LM10 model. The NanoSight LM10 counted the number of nanoparticles it tracked, counting as a number in the size distribution. These numbers are factored into the sample size.

A two-tailed t-test was conducted on the size distributions of three samples each of both curcumin-loaded and blank NLs. This t-test was conducted to determine the statistical significance between the mean diameter of the two distributions.

An f-test was also conducted on the size distributions of three samples of curcumin-loaded and blank NLs. The F-test was conducted to calculate statistical significance between the standard deviation in the mean diameter of the two distributions. The test was run with the alternate hypothesis that the blank NLs had a lower standard deviation than the curcumin-loaded NLs. The difference in standard deviations was found

to be statistically significant.

Langmuir Monolayer Studies. All Langmuir trough experiments were run multiple times for each experimental group: 4:1 PC:C (n = 5), 4:1 PC:C/Cur (n = 4), 1:1 PC:C (n = 6), 1:1 PC:C/Cur *(*n = 5), pure PC (n = 4), and pure PC/Cur (n = 7). Sample size differed between experimental groups due to omission of trials that were found to be outliers (± 1 standard deviation from the mean). All data are reported as mean ± standard error.

A two-tailed, unpaired t-test of unequal variance was conducted to determine the statistical significance between the average surface pressures of the control (monolayers with no curcumin added) and the experimental groups (monolayers mixed with curcumin). Statistical significance was determined at the confidence level of $p < 0.05$.

MTT Assay. All *in vitro* studies were conducted in triplicate. Three biological replicates were the completed per experiment and averaged for each figure. ANOVA was initially used to determine statistically significant differences at $\alpha = 0.05$.

A paired t-test was then conducted for all comparisons. Post-hoc analysis was also done after ANOVA using the Bonferroni correction at $\alpha = 0.003$. Cell viability was normalized with respect to the control groups that were not treated with any experimental conditions, defined as:

$$V = \frac{A_{exp}}{A_{con}},$$

where V denotes cell viability of the experimental condition of interest, A_{exp} its average absorbance, and A_{con} the average absorbance of the untreated control. Error propagation was carried out through usual sum of the squares:

$$\sigma_V^2 = \left(\frac{\partial V}{\partial A_{exp}}\sigma_{A_{exp}}\right)^2 + \left(\frac{\partial V}{\partial A_{con}}\sigma_{A_{con}}\right)^2,$$

where σ_x denotes the experimental error associated with the variable x. From the definition of V, we calculate the partial derivatives to obtain:

$$\sigma_V = \sqrt{(\frac{1}{A_{con}}\sigma_{A_{exp}})^2 + (\frac{A_{exp}}{A_{con}^2}\sigma_{A_{con}})^2}.$$

Reactive Oxygen Species Assay. The fold change in ROS fluorescence values was determined by:

$$F = \frac{R_2}{R_1},$$

where F is the fold change, R_2 the ROS values after the second step of each model, and R_1 the ROS values after the first step of the model. As with the cell viability from the MTT assay, we have an expression for the error on F as:

$$\sigma_F = \sqrt{(\frac{1}{R_1}\sigma_{R_2})^2 + (\frac{R_2}{R_1^2}\sigma_{R_1})^2}.$$

RESULTS

Aim I: Synthesis of the Curcumin-loaded Nanoliposomes

Microscopy. NLs were imaged under both brightfield and fluorescence in order to confirm the success of both the extrusion process and the attachment of the lissamine rhodamine B tag. Figure 6 shows that the extrusion process was able to transform the liposome solution from heterogeneous mixture of different sized particles (Figure 6a) to a homogenous solution of 200 nm nanoliposomes (Figure 6b). Uniform circular fluorescence was visible under fluorescence microscopy, confirming the successful production of NLs. Fluorescence was viewed under FITC filter to visualize the lissamine rhodamine B tag on the NLs (Figure 7). The NLs appeared to be discrete particles, signifying that the self-assembly into spherical liposomes was successful.

(a) (b)

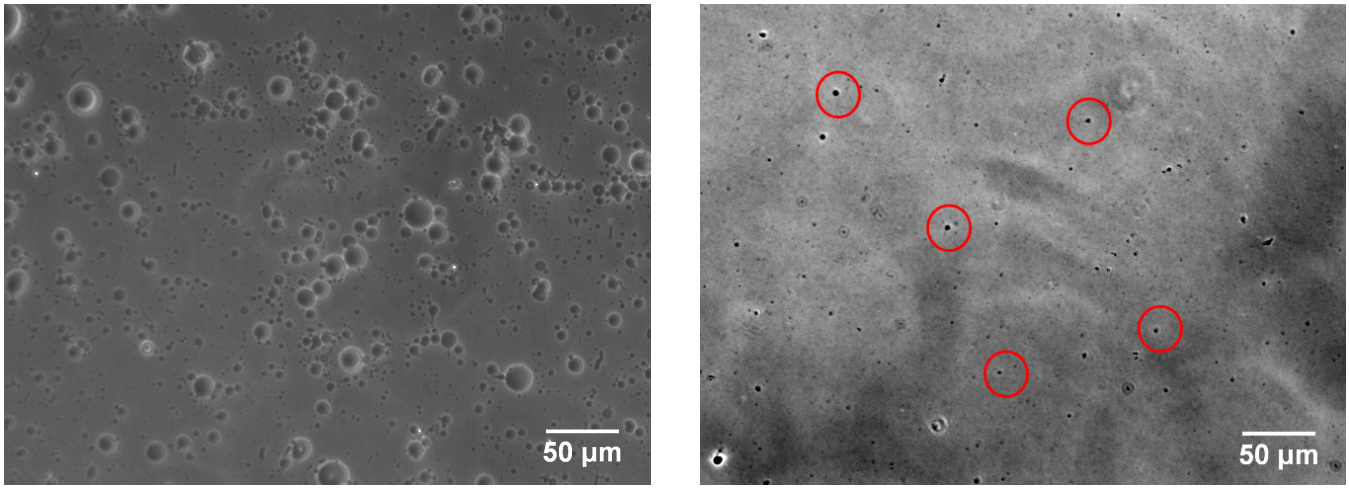

Figure 6. Images of curcumin-loaded NLs under brightfield microscopy. Liposomes were diluted 1:100 in glucose. (a) Nonextruded NLs (b) Extruded NLs.

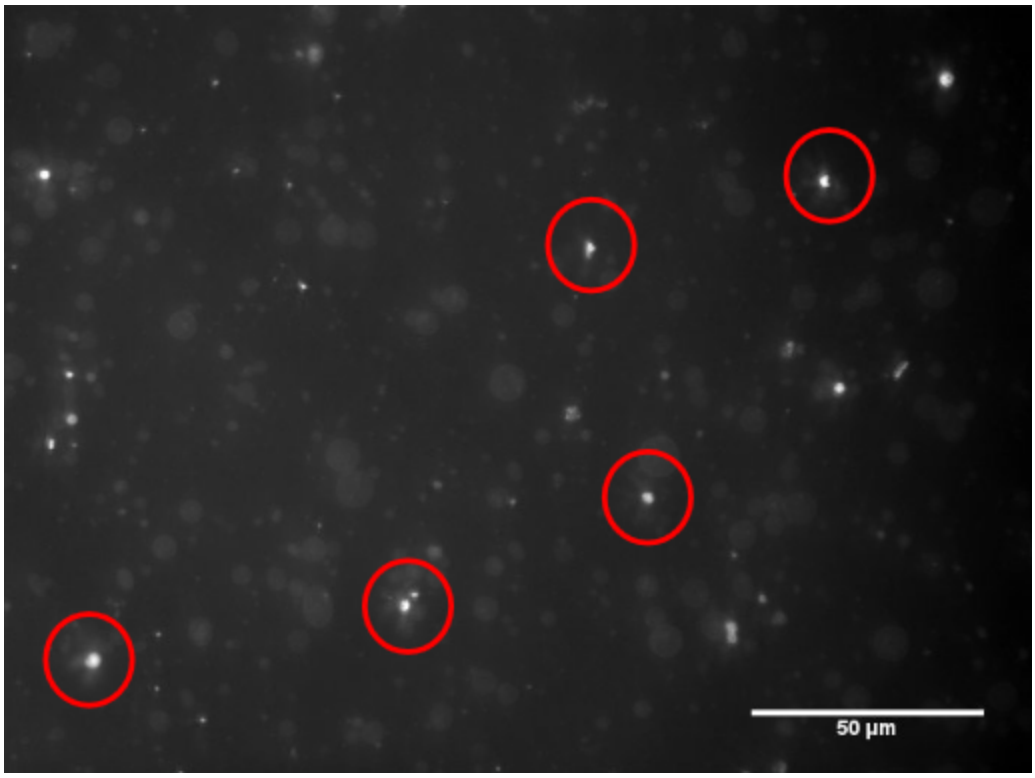

Figure 7. Image of extruded curcumin-loaded NLs using fluorescence microscopy. Lissamine rhodamine B tag on the NLs was visualized using FITC filter. NLs were diluted 1:100 in glucose for better visualization.

Size Distribution. Dynamic light spectroscopy was used to verify size distribution of our produced NLs. In measuring the size distribution of our NLs, we measured the extruded, homogenous liposome solution, which was diluted to 1:10000 to match the concentration range of the NanoSight LM10. From the data collected, we observed a size distribution, consistent throughout the various types of NLs created.

Size distributions were created for NLs both unloaded and loaded with curcumin. A sample size distribution graph can be seen in Figure 8. Over three trials, the mean diameter for empty NLs was 192 ± 57.7 nm, while the mean diameter for curcumin-loaded NLs was 224.67 ± 102 nm.

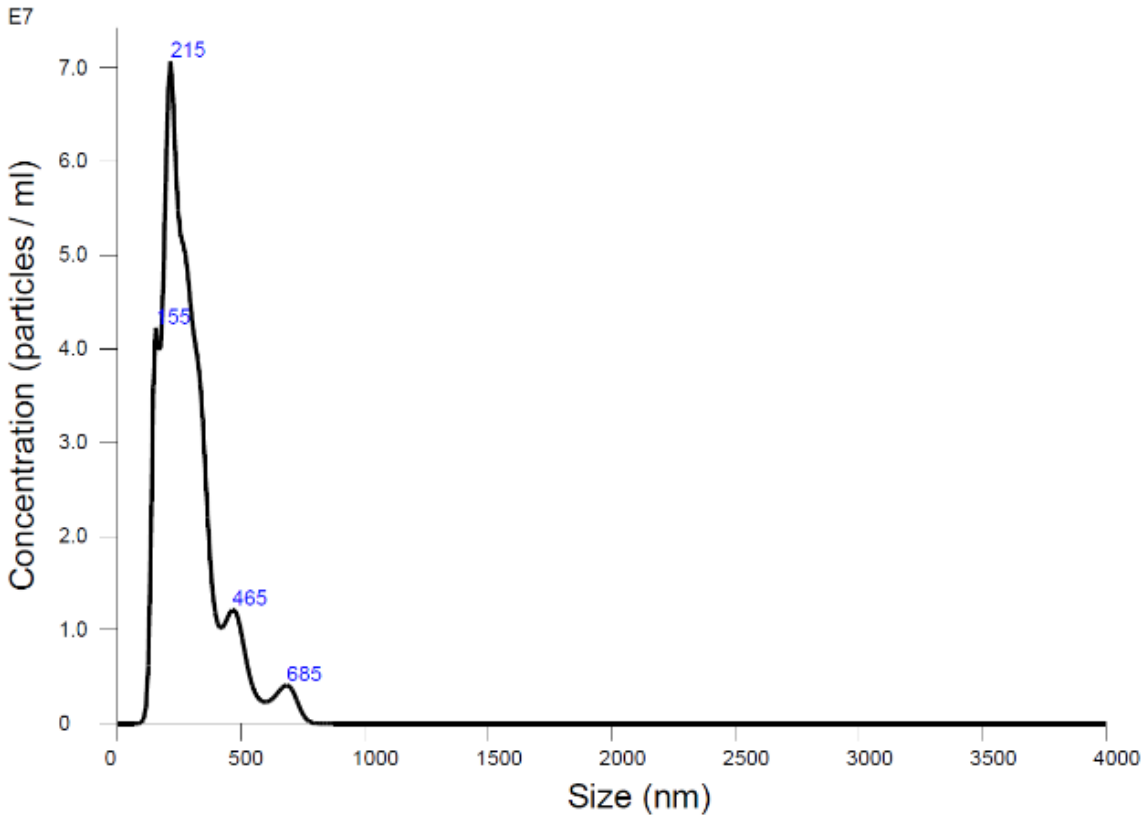

Figure 8. Sample size distribution graph of curcumin-loaded NLs. Sample was diluted at 1:10000 in sucrose.

Aside from the 4:1 PC:C ratio, size distributions were also measured for a 1:1 ratio, and at a half curcumin concentration, encapsulated in pure phosphatidylcholine. Over two trials, the 1:1 PC:C ratio generated a 222 nm diameter average, with a 98.5 nm standard deviation, while the half curcumin concentration in pure phosphatidylcholine, over three trials, produced a 200 nm diameter average, with an 89 nm standard deviation.

Encapsulation Efficiency. To calculate encapsulation efficiency of our NLs, we measured the absorbance of curcumin samples at 416 nm over three separate trials. From this data, we created a standard curve for curcumin in sucrose at 416 nm. A linear regression was applied to the resulting curve and a R^2 value of 0.9991 was obtained (Appendix D). This high R^2 value validated that we could use Beer-Lambert Law

calculations to measure encapsulation efficiency of our NLs. Over three trials, the calculated encapsulation efficiency averaged 2.55%, with a standard deviation of 0.158%.

Drug Retention Studies. In addition to general encapsulation efficiency trials, we also ran time-lapse encapsulation efficiency experiment over the course of fifteen days in order determine the drug retention properties of the NLs. Absorbance readings were taken in triplicate. We saw a strongly correlated ($R^2 = 0.994$) negative linear trend between encapsulation efficiency and time. By day 15, our NLs retained 79% of the originally loaded curcumin (Figure 9).

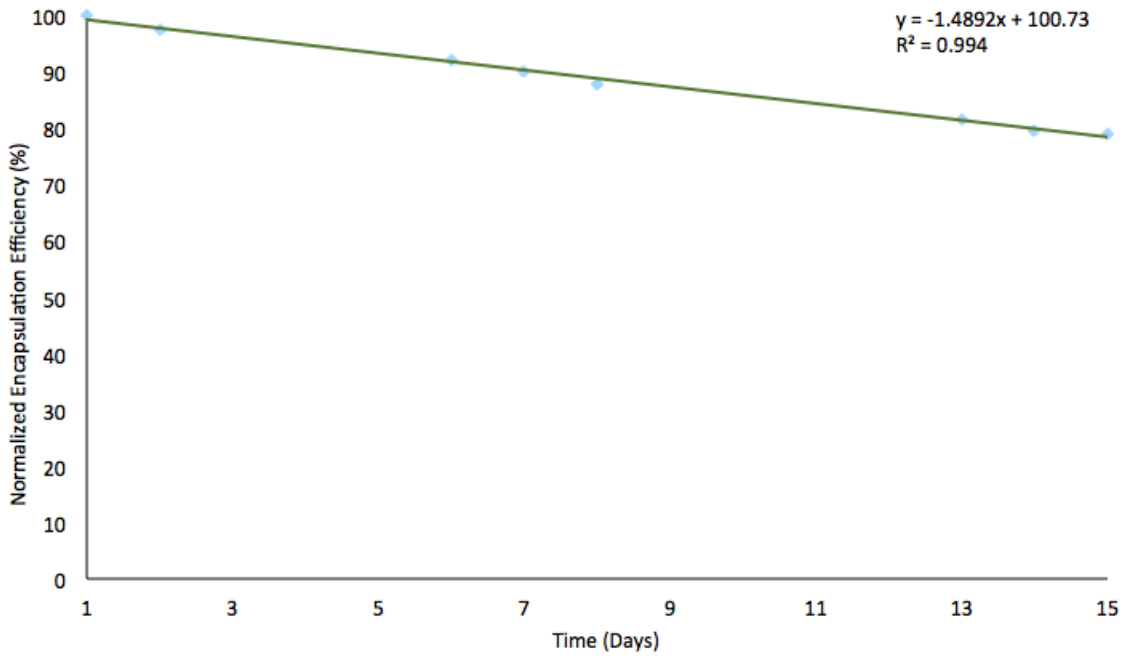

Figure 9. Concentration of curcumin retained within curcumin-loaded NLs over a period of 15 days, depicted in terms of encapsulation efficiency. All data was normalized to the encapsulation efficiency calculated on Day 1. Data is depicted as mean ± standard deviation (standard deviation was < 0.02 for all data points). *n=1*.

Langmuir Monolayer Studies. Figure 10 depicts the surface pressures in the mixture phosphatidylcholine and cholesterol monolayers at different PC:C ratios, and the same mixtures with added curcumin into the monolayers. Three ratios of PC:C were compared

to determine the effect of lipid composition on curcumin uptake. The 4:1 PC:C ratio was the only mixture where the surface pressure increased after the addition of curcumin. The average surface pressure for the pure 4:1 lipid monolayer was 33.7 ± 1.4 mN/m. Meanwhile, the average surface pressure for the mixed 4:1 lipid monolayer with curcumin was seen to have increased to 42.0 ± 1.3 mN/m.

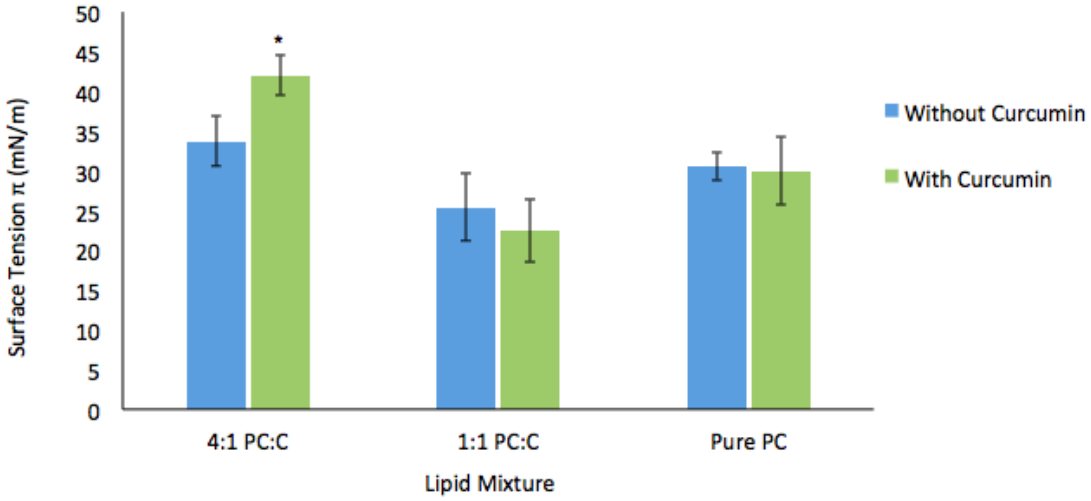

Figure 10. Comparison of average surface pressure π between lipid monolayers and mixed curcumin-lipid monolayers. Three different molar ratios of PC and C were compared. Data is depicted as mean ± standard error. PC: Phosphatidylcholine, Cholesterol. *p-value < 0.05 statistically significant when compared to pure lipid monolayer of the same mixture ratio. 4:1 PC:C (n = 5), 4:1 PC:C/Cur (n = 4), 1:1 PC:C (n = 6), 1:1 PC:C/Cur (n = 5), pure PC (n = 4), and pure PC/Cur (n = 7).

Both 1:1 PC:C and pure PC lipid composition showed a slight decrease in the surface pressures between the pure lipid and mixed monolayers. For the 1:1 PC:C pure lipid monolayer, the average surface pressure was 25.4 ± 1.7 mN/m which then decreased to 22.4 ± 1.8 mN/m with the introduction of curcumin to the monolayer. The pure PC lipid monolayer showed a similar trend. The pure lipid film had a surface pressure of 30.6 ± 0.9 mN/m while the mixed curcumin-lipid monolayer had a slightly lower surface

pressure of 30.0 ± 1.6 mN/m.

An unpaired, two-tailed t-test of unequal variance was used to evaluate the statistical significance of the incorporation of curcumin on the surface pressure. The test was run between the pure lipid and mixed curcumin-lipid monolayers of each mixture group. At $\alpha = 0.05$, only the 4:1 PC:C mixture was found to be statistically significant with a p-value of 0.0047.

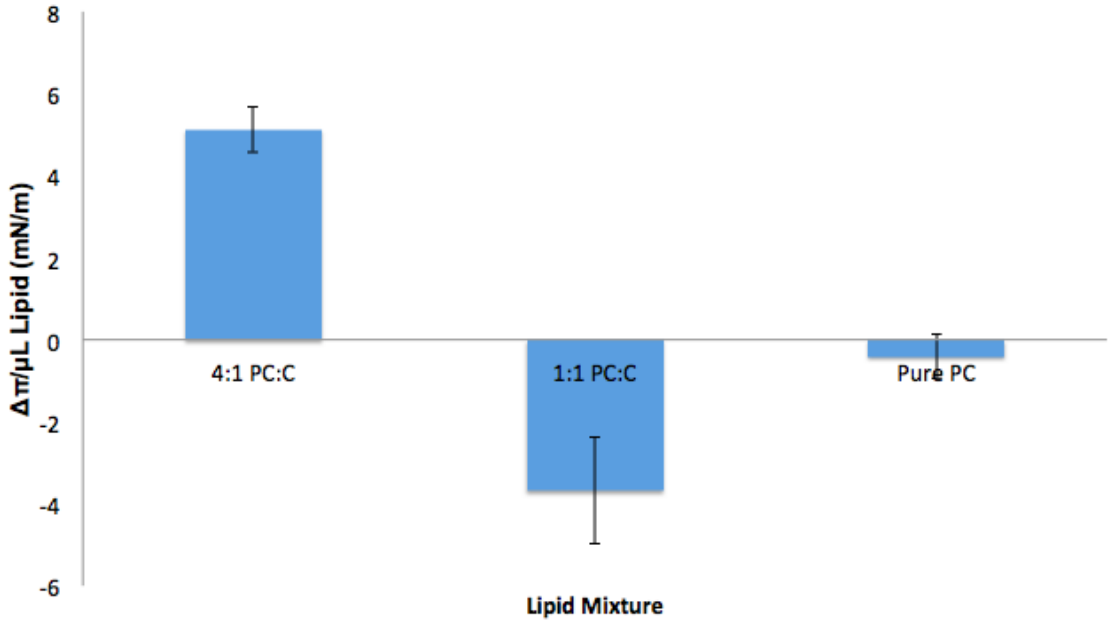

Figure 11. Change in average surface pressure per μL of lipid (PC+C) after the incorporation of curcumin for all three mixtures. Positive values indicate an increase in surface pressure after the addition of curcumin while negative values indicate a decrease in surface pressure. Data is depicted as mean ± standard error. Combining pure lipid and mixed curcumin-lipid monolayer trials, 4:1 PC:C ($n = 9$), 1:1 PC:C ($n = 11$), pure PC ($n = 11$)

In Figure 11, the change in the average surface pressures between the pure lipid film and mixed curcumin-lipid film was calculated by subtracting the mean surface pressure of pure lipid monolayer from that of the mixed curcumin-lipid monolayer. However, since the volume of lipid added for each trial was not consistent between the

different mixtures due to instrument constraints, the calculated surface pressure was normalized to the volume of lipid added in order to prevent skewed surface pressure data that may result from the weight of the lipid film itself. Positive values indicated an overall increase in surface pressure with the addition of curcumin while negative values showed a decrease in surface pressure. The greatest difference in surface pressure was observed in the 4:1 PC:C lipid composition, with a change of 5.13 ± 0.6 mN/m per μL of lipid. The 1:1 PC:C mixture showed a change of -3.68 ± 1.3 mN/m and the smallest change in surface pressure was seen in the pure PC at -0.41 ± 0.5 mN/m.

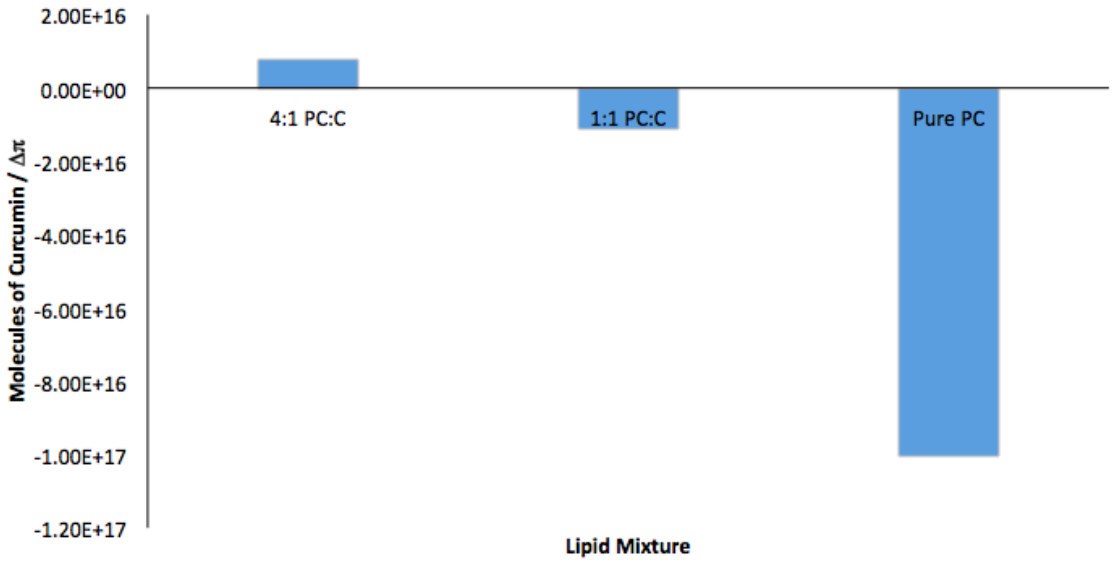

Figure 12. Number of curcumin molecules per average change of 1 mN/m for each lipid composition. A positive value indicates that the uptake of curcumin molecules causes an increase of 1 mN/m while a negative number indicates a surface pressure decrease of 1 mN/m. Combining pure lipid and mixed curcumin-lipid monolayer trials, 4:1 PC:C (n = 9), 1:1 PC:C (n = 11), pure PC (n = 11)

Figure 12 depicts the approximate number of curcumin molecules that has to be uptaken into by lipid membrane for the surface pressure to change by 1 mN/m. These values were calculated by dividing the known mass (and, by extension, the total number

of molecules) of curcumin added to the film mixture by the observed change in surface pressure that was shown in Figure 11. The obtained result was the number of curcumin molecules responsible for a change in 1 mN/m. A positive value indicated that the uptake of curcumin molecules causes an increase of 1 mN/m while a negative number showed that the uptake leads to a decrease of 1 mN/m.

Results showed that about 8.0×10^{15} molecules of curcumin led to an increase of 1 mN/m of tension in the 4:1 PC:C lipid mixture. A similar magnitude of curcumin molecules, about 1.1×10^{16} molecules, was responsible for the change in pressure for the 1:1 PC:C though it led to a decrease of 1 mN/m rather than an increase. Pure PC required the greatest number of curcumin molecules before a change of 1 mN/m in surface pressure could be observed. About 1×10^{17} molecules, which is almost 10 times more molecules than seen for the other two mixture ratios, were required to decrease the surface pressure by 1 mN/m.

Aim II: Testing the Curcumin-loaded Nanoliposomes in Cell Culture

The MTT assay was used to determine whether our curcumin-loaded NLs promoted cell viability in ARPE-19 cells. We tested the curcumin-loaded NLs' therapeutic potential in two ways: a preventative model and a treatment model. Additionally, we measured antioxidant activity using the ROS assay. We tested the curcumin-loaded NL's potential to reduce the production of reactive species in ARPE-19 cells.

In the preventative model, cells were pre-treated with the experimental conditions for 24 hours. Cells were then damaged for 24 hours with 600 μM H_2O_2. Studies have

shown that 600 μM is sufficient to induce oxidative damage in cells, and this time point has been used in several oxidative stress models to evaluate therapeutic efficacy (Kim et al., 2003). In the treatment model, cells were initially damaged for 24 hours with 600 μM H_2O_2 and then cells were treated with experimental conditions. MTT reagents were then added and assayed in both models. All data collected for the cell viability studies were normalized with regards to the cells that were untreated.

Optimization of Experimental Condition Parameters

Curcumin-DMSO Concentration. Optimization studies were first done to determine the concentration of curcumin-DMSO that should be tested for encapsulation purposes. To overcome the poor solubility of curcumin, we dissolved it in 1 mL of DMSO and verified that the concentration of DMSO used in this study would not affect cell viability. From our calculations, we determined that our curcumin solutions contained 4% DMSO weight/volume. In Figure 13, our optimization studies demonstrated that ARPE-19 cells treated with this concentration of DMSO had >95% cell viability ($p > 0.05$ when compared to untreated cells, indicating that there was no difference in viability the two conditions). As a result, we were able to ascertain that differences in cell viability were due to presence of the curcumin.

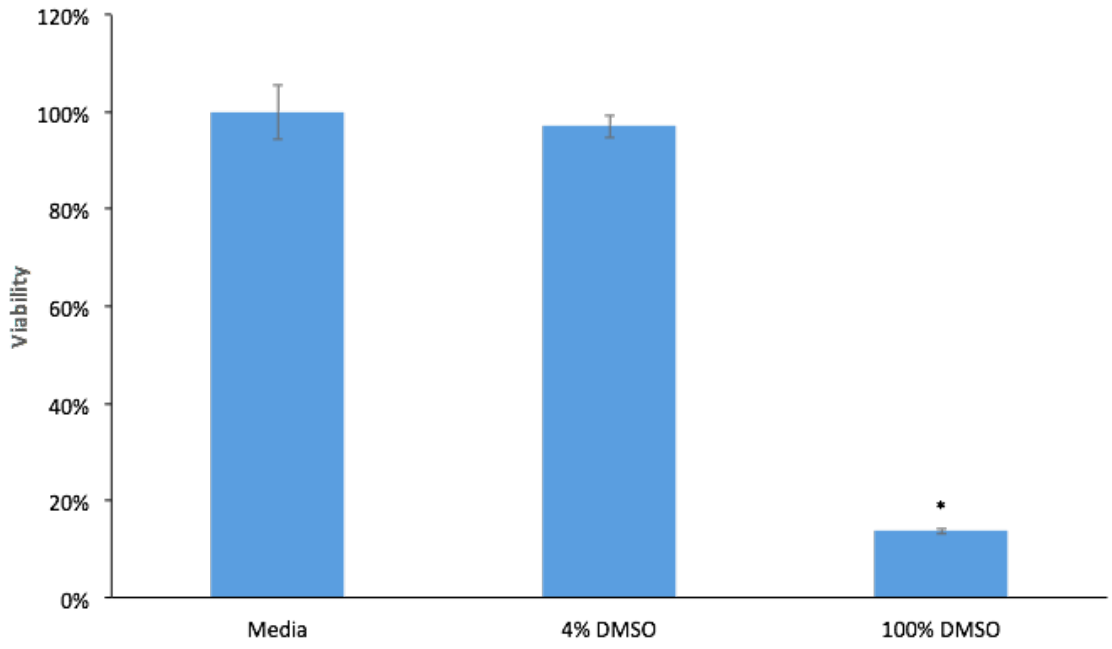

Figure 13. DMSO cell viability studies. Due to the poor solubility of curcumin, we reconstituted it in DMSO and tested to see whether the presence of DMSO would affect cell viability (* $p < 0.05$ when compared to basal media treated cells). *n=3* technical replicates and expressed as mean ± standard error)

After this, we then tested various concentrations of curcumin-DMSO. From these experiments, we determined that 10 µM of curcumin-DMSO ensured cell viability >60% (Figure 14). These results corresponded with literature values, which state that 20 µM of curcumin causes necrosis and cell death.

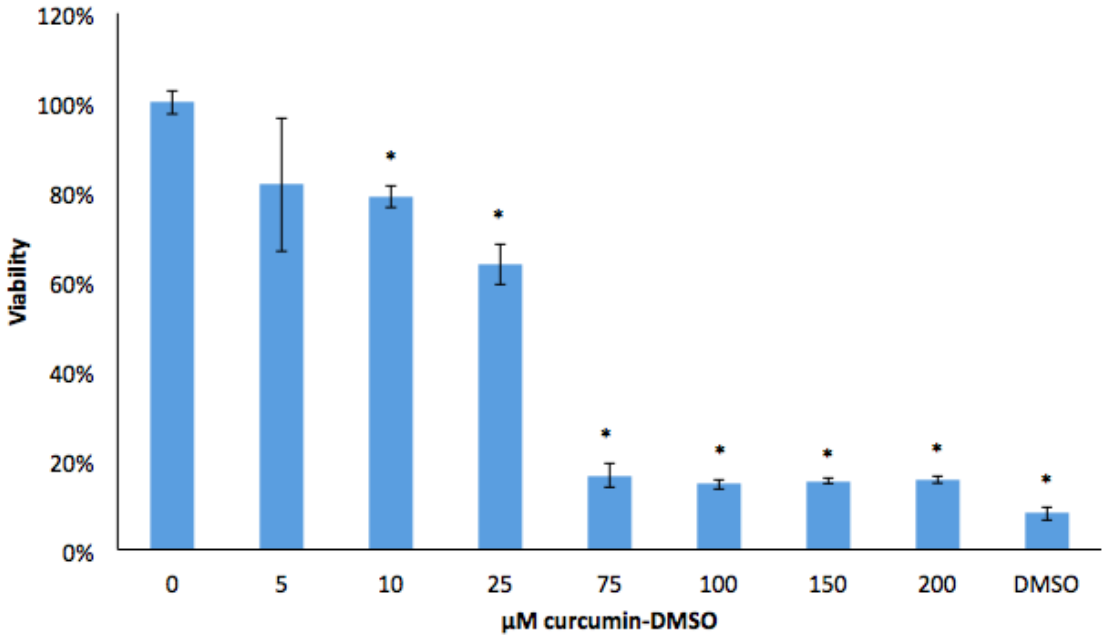

Figure 14. MTT Assay for Determining the Concentration of curcumin-DMSO needed for synthesizing the liposomal-curcumin complex. ARPE-19 cells were treated with varying concentrations of curcumin-DMSO for 24 hours. Plates were then assayed at this time point. Viability was normalized to the untreated cells. ANOVA gave $p < 0.05$ (* $p < 0.05$ when compared to untreated cells). *n=3* technical replicates and expressed as mean ± standard error)

Hydrogen Peroxide Concentration. 600 µM of H_2O_2 was determined to be optimal for inducing oxidative stress in ARPE-19 cells, as we retained >70% viability with respect to the untreated cells ($p < 0.05$). These results corresponded with previous literature values which demonstrated that 500-700 µM H_2O_2 was sufficient to induce oxidative stress in retinal cells (Figure 15).

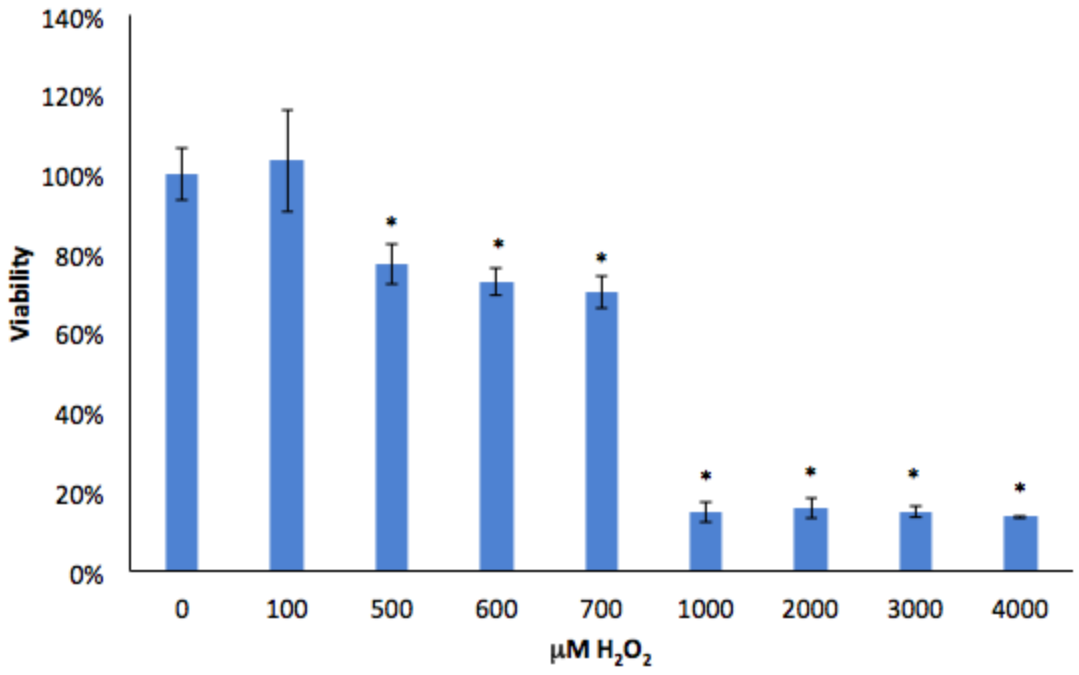

Figure 15. MTT Assay for Determining the Concentration of H_2O_2 needed to induce oxidative damage. ARPE-19 cells were treated with varying concentrations of $H_2O_2$for 24 hours. Plates were then assayed at this time point. Viability was normalized to the untreated cells. ANOVA: $p < 0.05$. (* - $p<0.05$ when compared to untreated cells). *n=3* technical replicates and expressed as mean ± standard error

Liposomal Mixture Dilution. We also verified that our curcumin-loaded NLs were not cytotoxic. As seen in Figure 16, optimization studies showed that our mixture of lipids maintained cell viability at >90% ($p > 0.05$ when compared to untreated cells). As a result, we were able to determine that differences in cell viability were due to the presence of the curcumin in the NLs.

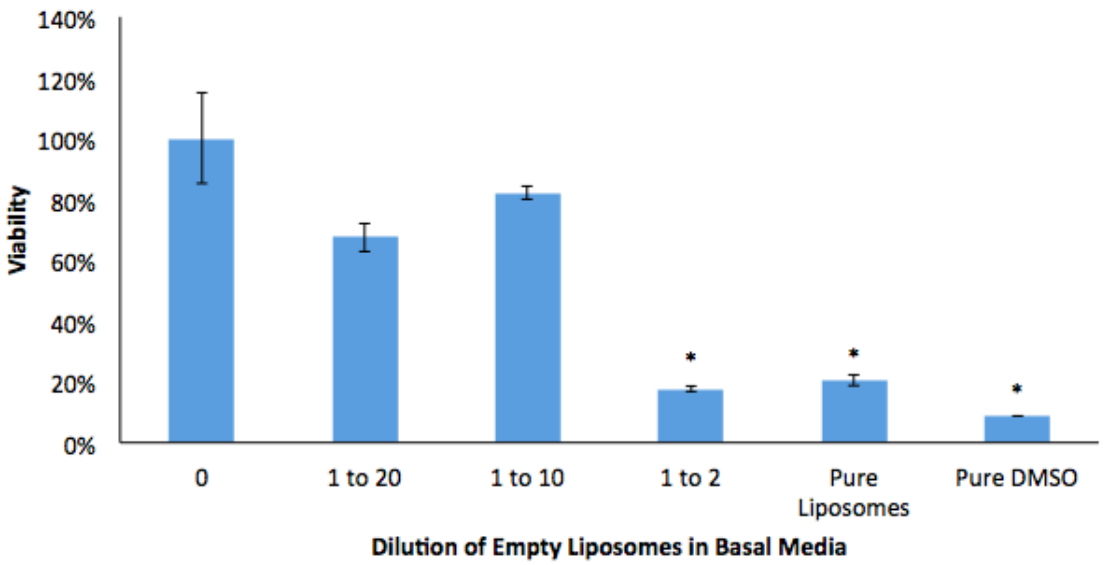

Figure 16. Viability of ARPE-19 cells when treated with varying dilutions of empty liposomes in cell media. Cell data was normalized with respect to lipid free basal media and assayed 24 hours after addition of experimental conditions. ANOVA: $p < 0.05$. (* $p<0.05$ when compared to untreated cells). *n=3* technical replicates and expressed as mean ± standard error

Time-lapse of Curcumin-DMSO. Several studies have demonstrated that high doses of curcumin result in cell death and apoptosis. As a result, for our studies, we decided to choose a dose of curcumin to encapsulate into curcumin-loaded NLs that, when uptaken into the cell, would not induce any cytotoxic effects. ARPE-19 cells were treated with 10 µM of free curcumin and imaged under brightfield for cell morphology. Figure 17 showed that cell morphology and viability changed considerably. Cells appeared to be undergoing blebbing, an indicator of apoptosis at 25 µM and 50 µM. These results were also quantitatively measured (Figure 14). Curcumin was seen to promote cell viability at low doses but caused cell death at high doses. ANOVA and t-test statistical tests demonstrated that these results were statistically significant ($p < 0.05$).

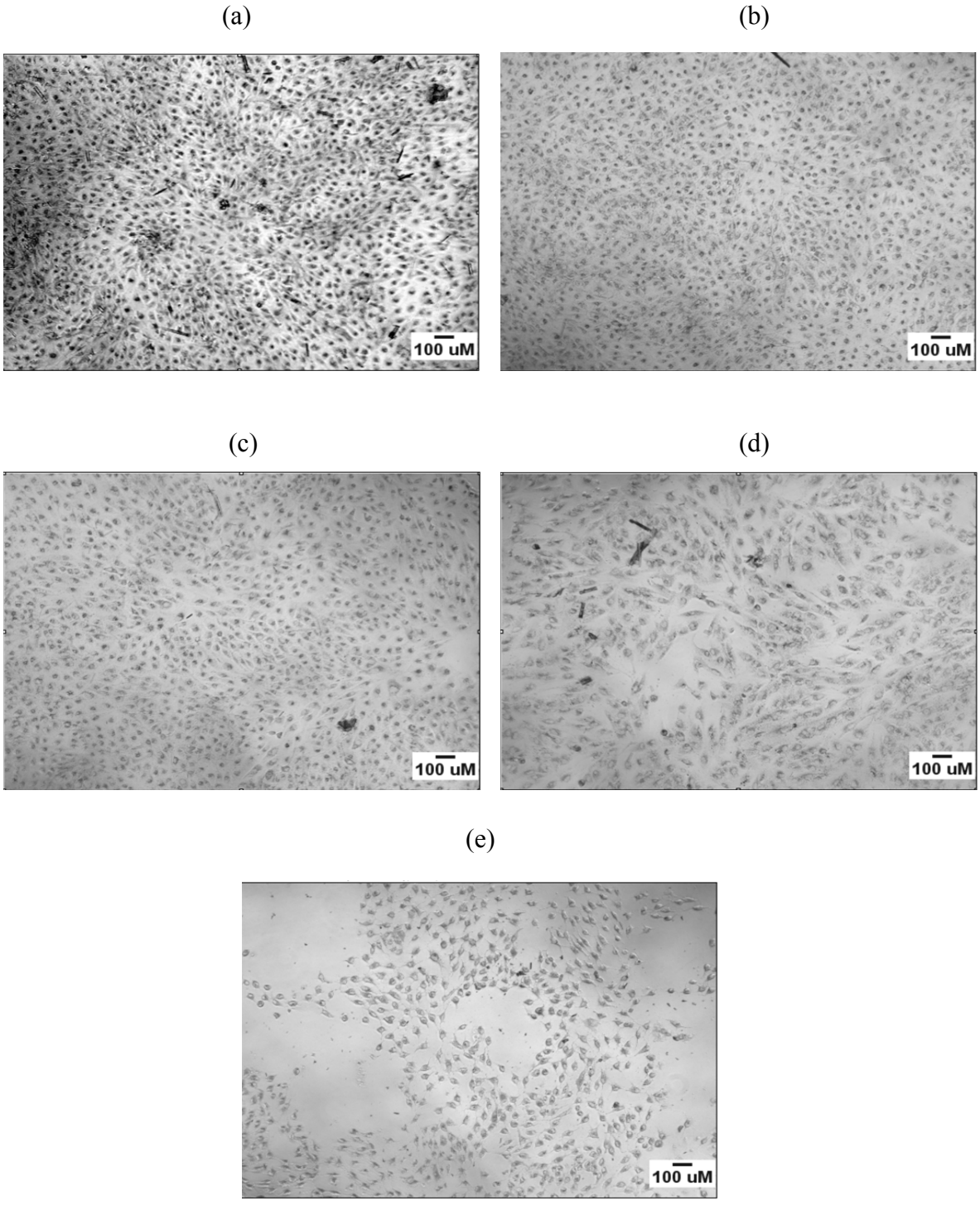

Figure 17. Representative brightfield microscopy images are also shown for a) 0 µM, b) 5 µM, c) 10 µM, d) 25 µM and e) 75 µM curcumin-DMSO at 10X.

Preventative Model. Due to the antioxidant and retinoprotective properties of curcumin, we decided to test our curcumin-loaded NLs in a preventative model. Cells were pre-treated with experimental conditions for 24 hours and then damaged with 600 μM of H_2O_2 for 24 hours.

MTT Assay. We were able to successfully damage cells with 600 μM H_2O_2, as cell viability reduced by 40%. In addition, viability reduced by 87% in the DMSO treated cells. Cell viability increased by 55% in the cells treated with curcumin-loaded NLs ($p < 0.05$) with respect to the untreated cells, indicating that our curcumin-loaded NLs may have potentially protected cells and promoted cell viability in general (Figure 18). However, since AMD is characterized by a buildup of oxidative stress, we compared the effectiveness of our curcumin-loaded NLs to cells that had undergone comparable oxidative stress. From these results, we found that cell viability increased by more than 60% ($p < 0.05$) with the addition of the curcumin-loaded NLs. These results suggested that our curcumin-loaded NLs could be beneficial in reducing some of the cytotoxic effects of oxidative stress. Due to curcumin's poor bioavailability, we decided to compare the effectiveness of our curcumin-loaded NLs to that of curcumin-DMSO. We demonstrated that cell viability increased by more than 50% ($p < 0.05$) in treated cells. However, the empty NLs also increased cell viability, as we demonstrated that viability increased by 26% with respect to the untreated cells. These results would need to be confirmed with further mechanistic studies regarding the curcumin-loaded NLs and liposomal mixture, and how it affects cell viability.

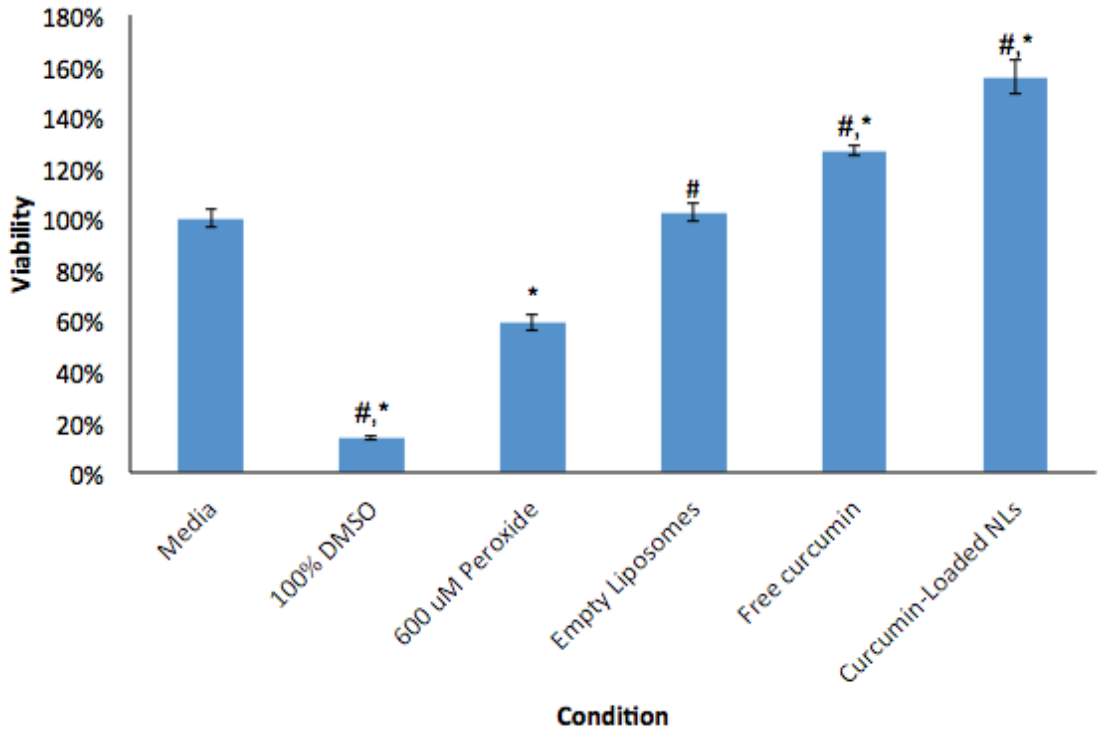

Figure 18: MTT assay of ARPE-19 cells after pre-treatment with liposomal-curcumin complex. Cells were pre-treated for 24 hours and then damaged with hydrogen peroxide for 24 hours. Plates were assayed after peroxide damage. Data was normalized with respect to cells treated with basal media and damaged. (# - $p < 0.05$ when compared to H_2O_2 treated cells. * - $p < 0.05$ when compared to curcumin-DMSO.) *n=3* replicates and expressed as mean ± propagated error

ROS Activity. Due to the increase in viability in the curcumin-NL condition, we decided to assay for antioxidant activity using the ROS assay. In this experiment, we assayed ROS levels before the addition of H_2O_2 and after the addition of it, in order to obtain a basal metabolic ROS level in these cells. As a positive control, we decided to use 600 µM H_2O_2, as it is a known producer of ROS. We used curcumin-DMSO as a negative control, since curcumin is a known reducer of radical species and an antioxidant. We then normalized the data with respect to the ROS levels before the addition of H_2O_2 and plotted as a fold change.

Our results demonstrated that we were able to induce oxidative stress

successfully. As seen in Figure 19, there was a 2-fold increase in the ROS levels with respect to the controls. We also demonstrated that ROS levels increased by 7-fold in the curcumin-DMSO cells. This suggested that although curcumin may be an antioxidant, its antioxidant activity could be impacted after the addition of peroxide. However, our curcumin-loaded NL treated cells showed that ROS activity increased by 2.5-fold. These results suggested that curcumin may be effective as preventative for oxidatively stressed cells in an encapsulated form.

With respect to the cells that underwent oxidative stress, there was only a 0.5-fold difference between these cells and our complex-treated cells. These results suggested that although we induced oxidative stress, our complex may not be as effective at preventing further damage. With regards to the curcumin-DMSO cells, there was a 4-fold change difference between these cells and the complex treated cells. These results showed that encapsulating curcumin may have allowed for us to reduce ROS levels better than if it were unencapsulated. Interestingly, the fold change difference between our control and complex was minimal, suggesting that the ROS bioactivity between the two samples was similar. These results further suggest that our complex may be more beneficial as a preventative measure.

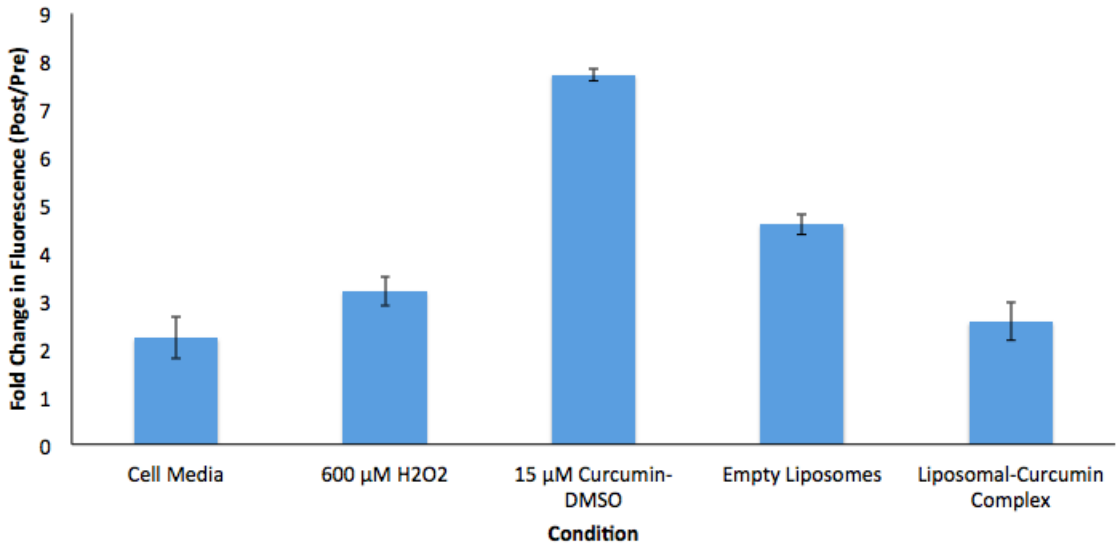

Figure 19. Fold change of ROS value when ARPE-19 cells were pre-treated with the liposomal complex. Cells were assayed for ROS values pre-damage and post-damage with hydrogen peroxide. Fold change was then calculated by dividing the post-damage ROS values by the pre-damage ROS values. *n=3* technical replicates and expressed as mean ± standard error

Treatment model

MTT assay. We also decided to test our curcumin-loaded NLs' ability to be used as a treatment for cells that had already undergone oxidative stress, as curcumin is known to affect this pathway. Cells were damaged with 600 µM H_2O_2 for 24 hours and then treated with experimental conditions as seen in Figure 20. Similar to the preventative model, we were able to successfully damage cells with 600 µM H_2O_2, as cell viability reduced by 40%. In addition, viability reduced by 85% in the DMSO treated cells. Cell viability increased by 28% in the curcumin-loaded NL treated cells ($p < 0.05$) with respect to the untreated cells, indicating that our curcumin-loaded NLs may be beneficial in promoting cell viability overall. With respect to the oxidative stress induced cells with no added treatments, we found that cell viability increased by 55% ($p < 0.05$). These results suggested that our curcumin-loaded NLs may be beneficial in reducing some of the

effects of oxidative stress.

However, we found that there was no statistically significant difference in cell viability between the cells that were exposed to the curcumin-DMSO and cells that were exposed to our curcumin-loaded NLs ($p > 0.05$, 8% increase in viability). Our results demonstrated instead that there was a statistically significant increase in viability between curcumin-DMSO and cells that were oxidatively stressed, indicating that curcumin has potential to be used as a treatment.

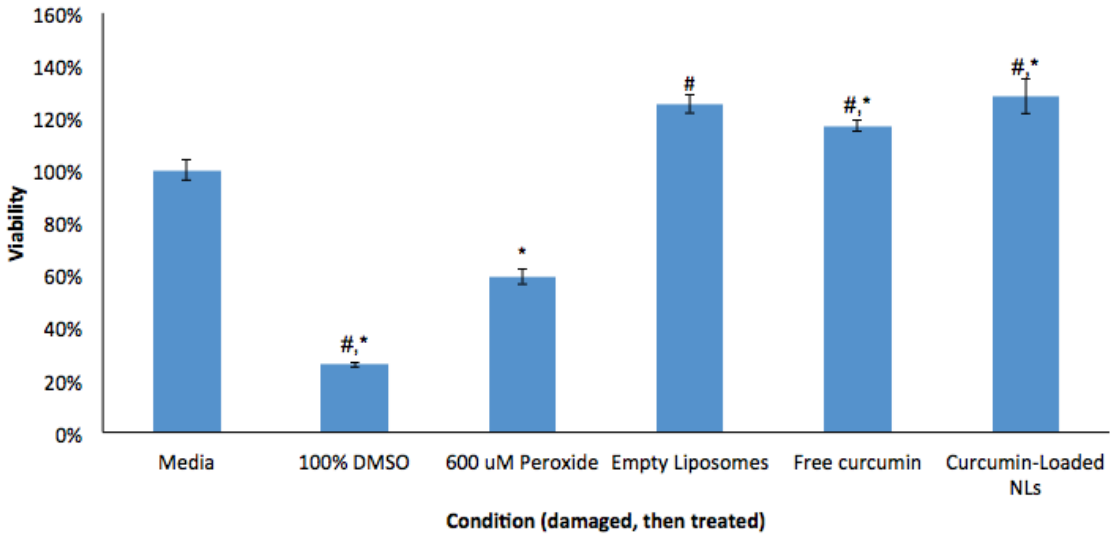

Figure 20. MTT assay of ARPE-19 cells after induction of oxidative stress with hydrogen peroxide. Cells were damaged with hydrogen peroxide for 24 hours and then treated with the liposomal complex solution 24 hours. Plates were assayed after treatments were applied. Data was normalized with respect to cells that were damaged and then treated with basal media. #$p < 0.05$ when compared to H_2O_2 treated cells. *$p < 0.05$ when compared to curcumin-DMSO.

ROS Activity. We assayed ROS levels after cells were treated with H_2O_2 and after they were treated with experimental conditions. As seen in Figure 21, there was a 0.45-fold increase in the ROS levels of the H_2O_2 treated cells, indicating that we were able to

induce radical production. However, compared to the fold changes observe in the preventative model, we found that our formulation did not cause as dramatic of a fold difference in the treatment model. There was a 0.1-fold difference between the control and curcumin-DMSO samples, indicating that the curcumin was able to affect antioxidant activity.

With respect to the peroxide treated cells, the curcumin-loaded NLs fold change difference was 0.1 lower. These results suggested that our complex may not have been as effective at reducing the ROS levels in cells that have already experienced oxidative damage. With respect to the curcumin-DMSO treated cells, our complex had a 0.05 lower fold change difference. Interestingly, the largest fold change difference was between the control and the complex (0.15). These results suggest that as a treatment, our liposomal complex may be less effective at inducing a large change in ROS activity than as a preventative.

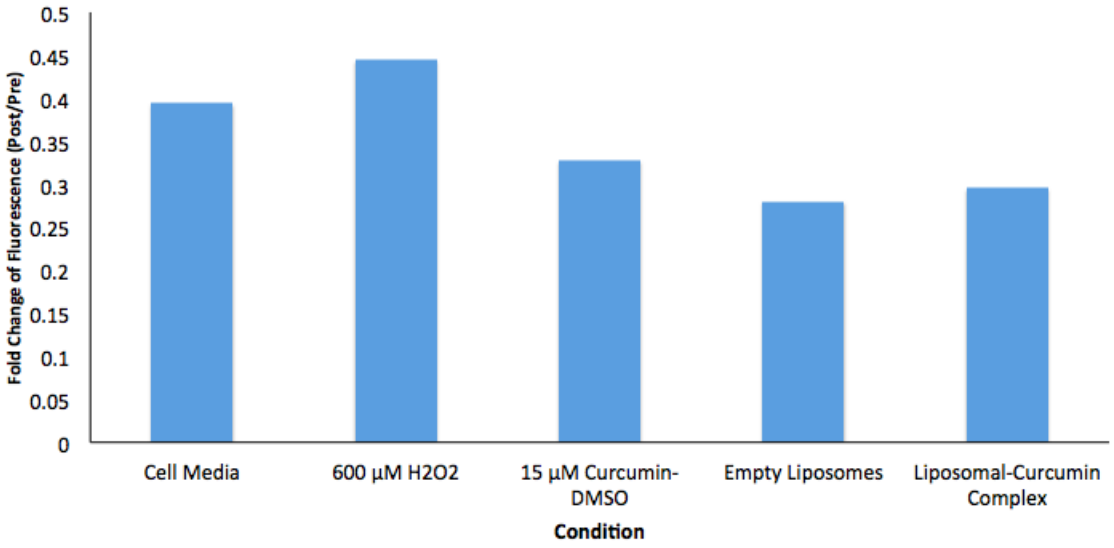

Figure 21. Fold change of ROS value when ARPE-19 cells were initially damaged with hydrogen peroxide. Cells were assayed for ROS values pre-treatment and post-treatment with the liposomal complex. Fold change was then calculated by dividing the post-treatment ROS values by the pre-damage ROS values. *n=1* replicate.

Aim III: Drug Delivery Testing

For *ex vivo* testing, we used a fluorescence microscope (Olympus IX71, Olympus Corporation) and a Franz diffusion cell to qualitatively observe the diffusion of the NLs through the retina and choroid of the eye at several time points. The curcumin-loaded NLs were allowed to pass through at 60, 135, and 210 minutes. After analyzing the microscopy images through ImageJ (Figure 22), we were able to image the fluorescent curcumin-loaded NLs, suggesting that they were able to successfully permeate through the layers of the posterior layers of the eye, namely the choroid and sclera.

There was not a discernable difference between the three images taken about an hour apart. We saw no major trend in the amount of fluorescent particles in the images. This suggested that hourly was too long of a time scale and that the NL concentrations had already reached near-steady state by the time we imaged.

For comparison, we also presented the diffusion of empty NLs through the eye (Figure 23). For this particular experiment, non-extruded NLs were used with a diffusion time of 180 minutes. Immediately, one can see that the faintly fluorescent background is not present in this image.

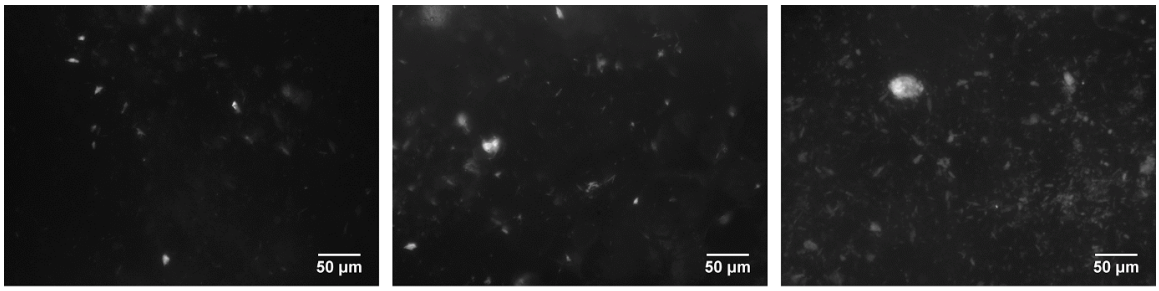

(a) (b) (c)

Figure 22. Fluorescence microscopy of the curcumin-loaded NLs diffused through the back of a porcine eye, with diffusion times of (a) 60 min, (b) 135 min, and (c) 210 min.

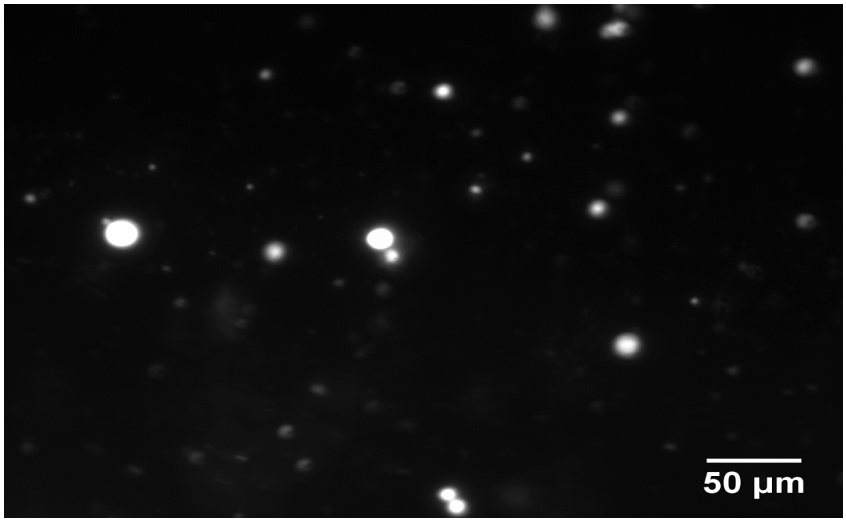

Figure 23. Non-extruded, empty NLs diffused through the back of a porcine eye for 180 minutes.

DISCUSSION

Age-related macular degeneration is a debilitating disease that affects millions of adults worldwide. It is primarily caused by the buildup of oxidative stress in the eye, causing the death of RPE cells in the retina and eventually leading to irreversible blindness. Curcumin, a powerful antioxidant derived from the spice turmeric, can be used as a potential therapeutic for the treatment and prevention of AMD. However, its clinical applications are currently limited due to poor bioavailability of curcumin, which makes it difficult to effectively deliver the drug to the back of the eye. In this current research, we aimed to improve the bioavailability of curcumin by loading it into curcumin-loaded NLs and show that it can increase cell viability and reduce oxidative stress in ARPE-19 cells.

Through our research, we were able to examine and analyze curcumin and its ability to be encapsulated within NLs, to retain antioxidant and retinoprotective properties after encapsulation, and its potential as an AMD treatment vs. prevention method. Additionally, we were able to determine the ability of the curcumin-loaded NLs to successfully reach the retinal layer of the eye.

Curcumin Encapsulation in Nanoliposomes

In pertinence to the size distribution experimentation, the results obtained suggest that when prepared in the same way, curcumin-loaded NLs are produced with approximately the same diameter as the empty NLs. There is a statistically insignificant difference between the diameters of curcumin-loaded and empty NLs using t-test statistical methods ($p > 0.05$). However, using an F-test, there is a statistically significant difference between the standard deviations in loaded and unloaded NLs, at the same

alpha level. A statistical comparison between the empty and curcumin-loaded NLs finds that the curcumin-loaded NLs have a higher standard deviation than the empty NLs. This statistical test shows that there is a greater variation, or less precision, in size distribution between our curcumin-loaded NPs and empty NPs

The NLs created have a wider size distribution than comparable extruded subjects: Liposome-Encapsulated Hemoglobin Blood Substitutes (LEHb). A paper by Arifin and Palmer (2003) on this subject used extrusion on LEHb, with a 200 nm filter, and created a monodisperse NL population, with distribution width of 20 nm. The thoroughness in extrusion used in this study may explain the ability to achieve a monodisperse size distribution. The study used successive extrusion steps, starting from higher diameter filters (10 passes each), and continuing the process with progressively smaller filters until the final filter, 200 nm, where 25 passes were performed (Arifin, & Palmer, 2003). Comparatively, our methodology uses 10 consecutive passes with the 200 nm filter only. The thorough extrusion process presented by Arifin and Palmer produces a more homogenous solution of nanoparticles.

From the Langmuir monolayer studies, the trends seen in Figure 10 suggest that, out of the three compositions tested, the 4:1 PC:C lipid mixture is the optimal ratio for maximum curcumin uptake. As shown in past studies, an increase in surface pressure indicates the inclusion of drug molecules, in this case curcumin, into the lipid monolayer. The 4:1 PC:C ratio was seen to be the only mixture that demonstrated this increase in surface pressure and, as such, is most suited for use when developing a liposome mixture for curcumin encapsulation. This is in accordance with previous literature where the presence of cholesterol has been seen to partially disrupt the packed phosphatidylcholine

structure to allow the insertion of curcumin molecules into the monolayer (Karewicz et al., 2011).

Both 1:1 PC:C and pure PC showed a slight decrease in surface pressure. Though not statistically significant in these present experiments, previous studies have shown that this observed decrease does have important implications on membrane stability. According to literature, this slight decrease suggests that there is possibly some desorption of lipid molecules (Gicquaud, Chauvet & Tancrède, 2003). The addition of the curcumin may have caused the partial collapse of the film into the subphase. In the case of the 1:1 PC:C specifically, the presence of cholesterol may have disrupted the phosphatidylcholine packing in a manner similar to what was seen with the 4:1 PC:C mixture. This disturbance may have contributed to the lack of surface pressure increase that marks curcumin uptake. Previous studies have shown the presence of cholesterol stiffens the lipid membranes and reduces drug permeability (Zhao & Feng, 2006; Liang, Mao, & Ng, 2004). In fact, increasing the cholesterol content in the monolayer has been shown to reduce the loading of poorly soluble drugs (Moghaddam, 2011). Due to the high numbers of cholesterol molecules, the film membrane may have been too impermeable to curcumin molecules, which may explain why the overall surface pressure did not increase. Furthermore, the high concentration of cholesterol in the mixture likely exhibited a strong ordering effect on the membrane (Karewicz et al., 2011). Despite its limited permeability, the introduction of even the smallest amounts of curcumin may have caused too much of a disturbance and loosened the packing structure, thus destabilizing the film. This subsequent desorption of molecules may have been reflected in the decrease of surface pressure.

The lack of curcumin uptake by the pure monolayer is also supported by previous studies. The packing structure of the lipids is already very relaxed without the stabilizing effect of the cholesterol. The addition of curcumin only further loosens the monolayer (Karewicz et al., 2011). This destabilization effect may have led to partial monolayer collapse and contributed to the observed decrease in surface pressure.

Figures 11 and 12 help to validate the destabilizing effects of curcumin. Figure 12 shows that the pure PC monolayer requires a greater number of curcumin molecules to affect surface pressure in comparison to the 1:1 PC:C mixture. This suggests that curcumin has a weaker destabilization effect on the pure PC than the other two mixtures. The pure PC mixture was also seen in Figure 11 to have the smallest decrease in pressure per volume of lipid, suggesting that the minimal decrease in surface pressure was actually due to the weaker destabilizing influence of the curcumin rather than the comparatively lower weight of lipid film itself, which is another factor that also could have contributed to the desorption of lipid molecules. Conversely, the positive values of the 4:1 PC:C mixture in Figures 11 and 12 suggest that the curcumin was successfully uptaken into the film and that any destabilization was counteracted by the ordering effects of the small amount of cholesterol present in the system.

Results of this present study, supported by conclusions of past research, have shown curcumin to have destabilizing effects on the lipid membrane. Based on these preliminary monolayer studies, a combination of phosphatidylcholine and cholesterol, specifically in a 4:1 ratio, has been shown to be the most effective of the three mixtures tested for stable curcumin uptake. Both too high of an amount and the complete absence of cholesterol have been shown to result in little to no positive effect on membrane

stability and curcumin uptake. Future studies would investigate different ratios of phosphatidylcholine and cholesterol ratios, such as 3:1 PC:C or 5:1 PC:C, in hopes of determining the ideal membrane composition for optimal curcumin uptake and vesicle stability.

In regards to encapsulation efficiency, low encapsulation efficiency of curcumin has been noted in previous studies. In a study by Takahashi et al. of curcumin loaded in lecithin nanoparticles, SLP-PC70 LEC showed an encapsulation efficiency for curcumin of 68.0 weight % while SLP-WHITE LEC encapsulated less than 10.0 weight %. (Takahashi et al., 2009). It is noted that curcumin has a high binding affinity to phosphatidylcholine (Began et al., 1999), therefore the 4:1 PC:C ratio was chosen to increase encapsulation efficiency. In a study by Chen et al., the encapsulation efficiency of different phospholipid curcumin-loaded NLs found encapsulation efficiencies over 80% for soybean phospholipids (SPC), egg yolk phospholipids (EYPC), and hydrogenated soybean phospholipids (HSPC) (Chen et al. 2012).

Though the encapsulation efficiency is markedly lower (2.55%) in this present research when compared to the aforementioned studies, the amount of curcumin encapsulated is nonetheless sufficient for the purposes of retinal drug delivery. RPE cells have a known upper dose threshold of 20 μM of curcumin (Hollborn et al., 2013) before cytotoxic effects set in. Taking this and the amount of curcumin added to the liposomal formulation into account, too high of an encapsulation efficiency would be unfavorable in terms of the delivered dosage. Furthermore, results from the *in vitro* studies show that the current amount of curcumin encapsulation still has a positive impact in increasing cell viability and reducing oxidative stress. Therefore, even with low encapsulation

efficiency, our curcumin-loaded NLs still show significant potential for use as a therapeutic for AMD. Additionally, our time-lapse encapsulation efficiency showed that the encapsulation of our curcumin-loaded NLs remained stable over a fifteen-day storage. This quality would be important to maintain for a pharmaceutical application.

Prevention vs. Treatment

In regards to the MTT assay, ARPE-19 cells treated with free curcumin (curcumin-DMSO), empty NLs, or the curcumin-loaded NLs all had a higher percent of viability and survival in comparison to the control cells that were just damaged with H_2O_2. Regardless of whether the cells were tested in the preventative model, in which damage with oxidative stress occurred after treating with the experimental conditions, or in the treatment model, in which oxidative damage was induced prior to treatment with the conditions, the results still yielded higher percent viability for those specific conditions mentioned above. This aligned with our hypothesis regarding the possibility of the curcumin-loaded NLs as a therapeutic for oxidative stress. Additionally, it showed that these curcumin-loaded NLs had no deleterious effects on the cells. However, there were slight differences in regards to percent viability between the two models.

In the treatment model, we were able to demonstrate similar results with this approach, as encapsulated curcumin appeared to increase cell viability with respect to free curcumin. This result is interesting, as not much data is available regarding curcumin's potential as a treatment for diseases, which involve oxidative stress. However, further studies need to be done to verify this result. Current literature suggests that there is strong evidence for curcumin to reverse oxidative stress damage, but not

much is known about the mechanism that this occurs by. Mirza et al. demonstrated that curcumin slowed the rate of ROS progression, and heme oxygenase 1 (HO-1) has also been implicated in the curcumin-induced reversal of oxidative stress (McNally, Harrison, Ross, Garden, & Wigmore, 2007). Assaying for biomarkers or changes in this pathway would also help us determine whether the increase in viability is due to changes in oxidative stress levels. Another approach to consider would be performing a similar panel of oxidative stress biomarkers, as oxidative stress is defined as changes in a variety of biomarkers. Potential biomarkers include protein carbonyl and DNA damage; an increase in oxidative stress is linked to high levels of protein carbonyl groups and to high levels of DNA damage (Dalle-Donne, Rossi, Giustarini, Milzani, & Colombo, 2003). Out of these two biomarkers, curcumin has been shown to influence DNA damage the most (Ayyagari et al.). Assaying for reversal or attenuation of DNA damage with this model would allow us to more conclusively determine how effective this curcumin-loaded NLs is at affecting oxidative stress levels.

In the preventative model, our results demonstrated that cell viability increased in the cells that were pre-treated with free curcumin as well as with the curcumin-loaded NLs. These results suggest that there may be some retinoprotective properties that allow for ARPE-19 cells to be protected from the oxidative damage that was induced by pulse delivery of H_2O_2. These results also correspond to similar studies done on other turmeric and curcumin derivatives, which have also been shown to increase cell viability in ARPE-19 cells. (Jitsanong, Khanobdee, Piyachaturawat, & Wongprasert, 2011; Hollborn et al., 2013). In these studies, both curcumin and their derivatives were also assayed for various antioxidant activity biomarkers. Antioxidant activity cannot be assessed through

a single biomarker, and as a result, a panel of biomarkers would allow us to assess whether our complex would be able to increase cell viability through an antioxidant mechanism, similarly to the multiple biomarkers associated with oxidative stress. Potential biomarkers include superoxide dismutase and glutathione peroxidase, as demonstrated by Jitsanong et al. (2011) for assaying the antioxidant activity of curcuminoids.

In the preventative model, there was a more prominent difference in cell viability between the empty liposome and the curcumin-loaded NLs on the ARPE-19 cells than that of the treatment model. This suggests that the curcumin-loaded NLs could be more beneficial as a preventative method rather than a treatment for AMD. Unexpectedly, it was also observed that cells treated with just empty nanoliposomes also increased percent viability in a similar manner as the curcumin-loaded NLs in both the preventative and treatment models. Specifically in the treatment model, there was no significant difference in percent viability between the empty NLs and curcumin-loaded NLs, which may either suggest a possibility of therapeutic properties from the mixture of lipids and agents utilized to construct these NLs or reflect poor encapsulation efficiency of these NLs. Phosphatidylcholine, the primary component of the NLs, have been shown to possess some antioxidant properties in previous studies. Ghyczy et al. (2008) found that phosphatidylcholine metabolites help to inhibit the production of ROS in a small bowel organ model, suggesting that phosphatidylcholine does have significant antioxidant properties. Phosphatidylcholine also exhibited antioxidant properties *in vivo* in rat models. Demirbilek et al. (2004) found that polyenylphosphatidylcholine, a derivative of phosphatidylcholine, significantly decreased levels of MDA (a biomarker of oxidative

stress) in rat tissue while Lee et al. (2013) saw that phosphatidylcholine ameliorated renal toxicity in rats by enhancing antioxidant enzyme activity such as that of superoxide dismutase. Previous studies have also shown the potential of cholesterol, the other main component of the NLs, to act as an antioxidant in rats. For instance, one study found that increased cholesterol in rat liver cells increased the activity of catalase, which prevents the formation of lipid peroxidation (Mahfouz and Kummerow, 2000). A similar study found that cholesterol in rat liver cells increase the activity of the enzyme GSH-Px, which also prevents the formation of lipid peroxidation (Yuan, Kitts, and Godin, 1998). An additional study found that diets high in cholesterol reduced lipid peroxidation in the liver and red blood cells of rats (Yuan and Kitts, 2003). These studies show that cholesterol may have moderate antioxidative properties, which could explain why there was no significant difference in percent viability between the empty NLs and curcumin-loaded NLs.

Retention of Antioxidant Properties

In order to demonstrate that our curcumin-loaded NLs are effective at increasing antioxidant activity, we measured the reactive oxidative species levels *in vitro*. This approach is frequently used as a preliminary screening to determine whether there is antioxidant activity in general present in cells that are treated with various compounds. A lower level of reactive species indicates that there may be some other antioxidant activity that the cell is undergoing due to a therapeutic.

From our results, we demonstrated that there was a reduction in the relative levels of reactive oxidative species overall when the ARPE-19 cells were treated with our

curcumin-loaded NLs. In conjunction with our cell viability studies, these results showed that our curcumin-loaded NLs increased cell viability through an antioxidant pathway. As this concentration of curcumin is known to cause damage, and we observed that there was both an increase in viability and a reduction in ROS, there may be reason to believe that encapsulating the drug attenuates the overall cytotoxic effect. While the ROS assay measured the general trends of ROS levels, more specific mechanisms could be targeted as well. These specific substrate tests would need to be done in conjunction as study results feature discrepancies regarding the effect of superoxide dismutase, a certain enzyme, on antioxidant activity (Sharma et al., 2013; Jia et al., 2011; Yildirim, Ucgun, & Yildirim, 2011). However, further studies could verify and better understand this process. For instance, time lapses could be performed to determine whether ARPE-19 cells would die after prolonged exposure. These findings agreed with similar studies that were done to encapsulate curcumin as well. For example, Jithan et al. demonstrated that the release of curcumin can be controlled through the use of albumin-nanoparticles. Cyclodextrin has also been used to encapsulate curcumin in the food industry, however, there is limited research about curcumin encapsulation for the treatment or prevention of retinal degenerative diseases (Mangolim et al., 2014). These results show the potential to prevent damage in these types of diseases.

We also tested whether antioxidant activity would be altered by curcumin in a treatment model. These results, when compared to the preventative model, showed that the antioxidant effect of curcumin was not as prominent when the cells were already damaged. This may suggests that curcumin-loaded NLs may be not be impacting antioxidant pathways directly, but rather alternate pathways, such as oxidative stress

pathways, when used post-oxidative stress; this corroborates several other studies that emphasize curcumin's ability to protect and prevent damage from oxidative stress, rather than treat it. Our results show that there is potential for these curcumin-loaded NLs to be used as a treatment but their effects may be less pronounced. Further studies measuring ROS levels throughout the course of the experiment could help clarify this distinction.

Mechanism of Nanoliposome Uptake and Curcumin Intracellular Trafficking

By elucidating the exact mechanism of liposome uptake by the RPE cells, the data from our *in vitro* studies can be better understood in the context of liposomal drug delivery and AMD treatment. The cellular uptake of liposomes is thought to occur in two ways: endocytosis and membrane fusion (Düzgüneş & Nir, 1999). As ARPE-19 cells are known to uptake liposomes via endocytosis (Peyman, Schulman, & Neisman, 1995; Neisman, Peyman, & Miceli, 1997), only endocytosis will be further discussed. Endocytosis occurs as the cell membrane engulfs a specific macromolecule in an intracellular membrane-bound vesicle, known as the endosome, which is then trafficked through the cells, possibly through use of microtubules (Glover, Glouchkova, Lipps, & Jans, 2007), to lysosomal compartments (Straubinger, Hong, Friend, & Papahadjopoulos, 1983) and ultimately to a final destination. In the case of curcumin-loaded NLs, the target is the mitochondria, the location where the curcumin is known to modulate lipid peroxidation (Zingg et al., 2012). Previous studies have detailed the liposome uptake in a variety of cells, thus highlighting the numerous biochemical and physical factors that facilitate or inhibit endocytosis. Kang, Jang, and Ko (2017) investigated the endocytotic uptake of liposomes by fibroblasts and glioblastoma cells. They found that the uptake of

liposomes is dependent on surface charge, as cationic liposomes were internalized more quickly when compared to anionic and neutral liposomes. Similar results were obtained in studies by Dan (2002), Li et al. (2011), and Soenen, Brisson, & De Cuyper (2009). It was theorized that the electrostatic interactions between the cationic surface of the liposomes and the negatively charged cell membrane brought the two membranes closer together, allowing for increased endocytotic uptake (Elouahabi & Ruysschaert, 2005). These same electrostatic interactions had an opposite effect on the anionic liposomes, where the same-charge repulsion hindered liposome proximity and subsequently cellular uptake (Honary & Zahir, 2013). Nevertheless, several studies (Hong & Papahadjopoulos, 1992; Bajoria, Sooranna & Contractor, 1997) have found that negatively charged liposomes were able to be endocytosed regardless of the electrical repulsion. This suggests that the presence of cell receptors and the subsequent ligand-receptor bonding can overcome the repulsive electrostatic interactions. Regardless, most, if not all, studies agreed that charged liposomes had greater cellular uptake via endocytosis than neutral liposomes. This has significant implications for the cellular uptake of our curcumin-loaded NLs. Made of phosphatidylcholine and cholesterol, these liposomes are mostly neutral. As suggested by the previous studies, the lack of a surface charge greatly limits the uptake of the NLs by the ARPE-19 cells. This is potentially reflected in the less pronounced impact of the curcumin-loaded nanoliposomes on lowering ROS activity compared to the free curcumin. It is likely that with the addition of surface charge like poly-l-lysine or with the replacement of phosphatidylcholine with a charged lipid such as 1,2-dioleoyl-3-trimethylammonium-propane (DOTAP), the NL uptake would greatly increase and we would see a greater difference in ROS activity between the loaded NLs

and the free curcumin. Additionally, lipid composition outside of electrical charge has been seen to enhance the endocytosis of the liposomes. In a study by Lee et al. (2013), liposome uptake by Schwann cells, endothelial cells, and neural cells via endocytosis all increased by 5-,11-, and 8-fold after the addition of cholesterol to the liposome composition. To our knowledge there are no similar data with regards to specifically ARPE-19 cells but the Lee et al. (2013) study suggests that there could possibly be a similar effect on the endocytosis of our curcumin-loaded NLs by the ARPE-19 cells. There is a possibility that the addition of more cholesterol to liposome composition could increase cellular uptake, resulting in a greater and more prominent reduction of ROS activity when compared to the free curcumin.

Metabolic Trafficking of Curcumin. Curcumin affects several metabolic pathways in the cell. It primarily affects cholesterol accumulation and the glutamate transporter. Studies have shown that curcumin treated cells tend to have reduced cholesterol accumulation . This was seen in Zhao et. al (2012), as they were able to demonstrate that higher levels of curcumin resulted in the overexpression of cholesterol efflux biomarkers such as PPARγ, LXRα, and ABCA1. However, these studies interestingly note that curcumin has a limited effect on other lipid metabolism genes such as ACAT-1 and 15-LOX (Zhang et. al, 2014). Future studies involving curcumin and retinal oxidative stress should probe for the cholesterol accumulation biomarkers, as there is limited research available on how it affects ARPE-19 lipid metabolism.

In addition to the cholesterol metabolism pathways, curcumin also affects the glutamate transporter – GLT1 (Zhang et al., 2014). GLT-1 is known to be involved in antioxidant activity, as lower levels of it are associated with high levels of antioxidant

activity and reduced neurotoxicity in cells. There is also limited research available on GLT-1 expression in ARPE-19 cells. By assaying for this transporter, and determining the relative transporter activity when cells are treated with the curcumin-loaded NLs, we may be able to better understand the pathway that this complex takes *in vitro*.

Another aspect to consider in curcumin trafficking is RPE65. RPE65 is a protein that is involved in the pathogenesis of AMD. Studies have shown that overexpression of RPE65 causes AMD (Redmond et. al, 1998) . As a result, inhibiting its activity may potentially result in a slower rate of progression. By probing for RPE65 activity in curcumin treated ARPE-19 cells, we may be able to determine whether curcumin's retinoprotective properties affects AMD development.

Nanoliposome Permeability and Release

Our drug delivery model demonstrated that curcumin-loaded liposome nanoparticles can effectively permeate the scleral and choroidal layers of porcine eyes to ultimately reach the retina. Through experimentation with the Franz diffusion cell, we were able to simulate a pressurized system similar to that of *in vivo* eyes. Our results indicate, qualitatively, that encapsulating curcumin in NLs allows for the permeability of curcumin. However, the qualitative nature of our study does not allow for precise conclusions about the diffusion process. In particular, though we observed an increase in fluorescent intensity from our time-lapse images, we offer no estimate on the diffusion coefficient.

On a cellular level, it is more difficult to evaluate NL permeation and release, as only the lissamine rhodamine B tag is directly visualized. The lissamine fluorescent tag is

known to bind tightly to encountered cell filaments, so we may only track the NL as far as the cell membrane where the lissamine tag and NL contents theoretically separate (Sanger, Mittal, & Sanger, 1984). Once the NL permeates into the cell lipid bilayer, it partitions based off the difference in solubility between the bilayer and the cytoplasm (Kubinyi, 1979).

We also note a difference between empty and curcumin-loaded NL in fluorescence images. In particular, the empty NLs have much more well-defined shapes, as opposed to the curcumin-loaded NL images. We are confident that this is not an artifact of the imaging process; rather, it appears that the NLs aggregate when formed with curcumin, a phenomenon that we also observed in our cell culture microscopy studies. Surfactants can be used to increase a molecule's effective solubility. However, any use of surfactants should not create a disadvantageous loss in permeability, as the effectiveness of a drug is dependent on both (Dahan & Miller, 2012).

Although the results do not allow us to fully characterize the curcumin-loaded NLs' ability to be implemented via a topical application, such as an eye drop, we are able to conclude that it has the ability to permeate the tissues and protein junctions between the sclera and choroid. In order to draw more accurate and viable conclusions about the NLs permeability and diffusion characteristics, future experimentation would require a shortened time scale wherein data are collected in shorter periods than the hourly scale used in this study.

Limitations

In this study, we have demonstrated the potential of our curcumin-loaded NLs as

a preventative measure, though there are still several considerations with our results. We decided to model the oxidative stress that induces AMD is through a pulse delivery of H_2O_2. This approach has been shown in several studies to be a reliable way to model AMD, however, AMD is characterized by constant oxidative stress, not an isolated event. In order to demonstrate the effectiveness of the curcumin-loaded NLs in a more realistic AMD model, we would need to use a system that could constantly generate H_2O_2. For example, glucose oxidase and glucose have been used in conjunction to constantly produce peroxide. In a study conducted by Graf and Penniston (1980), the researchers demonstrated a colorimetric method to quantify glucose by measuring hydrogen peroxide produced from the glucose through glucose oxidase catalysis. Determinations of glucose concentrations with glucose oxidase produced hydrogen peroxide in a yield of 73.9% of theoretical, and this oxidation yield is substantial enough for consistent reproducibility. By doing so, we would be able to more conclusively say that our curcumin-loaded NLs could be used to attenuate the effects of AMD. Another limitation is the experimental design as an *in vitro* study. Although it is the logical approach to testing a new compound, it limits our ability to make predictions about the *in vivo* effect of our curcumin-loaded NLs. There are other cell types and layers that the treatment would need pass through or interact with, which may impact what concentration reaches the retina. A quantitative *in vivo* study would be able to demonstrate the therapeutic's feasibility to penetrate the various layers of the eye and exert a therapeutic effect.

Another major consideration is drusen levels. Clinically, dry AMD's pathology is defined as and characterized by the buildup of drusen in the retinal layer. In this study, we primarily assayed levels of various oxidative stress and antioxidant activity

biomarkers. By assaying for proteins and lipids that are present in drusen, we would be able to conclusively determine whether our curcumin-loaded NLs have a clinically significant effect on the progression and development of AMD; these studies could be performed *in vitro* before progressing to an animal model of AMD.

One of the major limitations of the *ex vivo* testing was the suboptimal choices of fluorescence. As previously mentioned, the excitation wavelength for curcumin is 424 nm (Kunwar, Barik, Priyadarsini, & Pandey, 2007) while that of the rhodamine tag used is marketed at 560 nm. However, we found that the intensity of curcumin's fluorescence is far too low to be imaged by our equipment, which was equipped with the FITC-TRITC filter combination (485 nm and 550 nm, respectively). The excitation spectrum of curcumin is too narrow to fluorescence significantly under the 485 nm FITC light; rather, we observed that the rhodamine tag still fluoresces under the blue light, although much more faintly.

Ex vivo testing with the Franz cell was originally intended to collect quantitative data by determining the concentration coefficient between the original solution and the receptor solution. However, the UV-vis spectrometer available through the school was not sensitive enough to detect the small concentrations of either curcumin or NLs (via the rhodamine tag). This was mainly due to the large volume of the receptor chamber (5 mL) of the Franz cell compared to the concentrations obtained by the curcumin-loaded NL synthesis process.

CONCLUSION

Our experimentations revealed that curcumin can successfully be encapsulated within NLs and increase cell viability in both preventative and treatment applications. Additionally, we conclude that the curcumin-loaded NLs have the potential to permeate through the posterior portion of the eye in order to reach the retina and exert an antioxidative effect.. While our results are promising in answering our research question, they are preliminary findings and therefore provide the foundation for future studies in pharmaceutical research. Such studies could remediate our limitations in order to make more statistically significant conclusions.

Future investigations would focus on clinical translations of our approach and involve *in vivo* studies to prove that a topical solution can reach the posterior layers of the eye as well as deliver a therapeutic amount of curcumin. In conjunction with *in vivo* testing in animal models with AMD, additional surface modifications to the NLs could be added to the protocol to better aid both specificity and affinity of to retinal cells. Future studies would also require the development of a carrier solution for optimal drug delivery and tolerance. Ultimately, our study may lay the foundations for development of a non-invasive option for AMD prevention and treatment.

REFERENCES

Age-Related Eye Disease Study Research Group. (2001). The Age-Related Eye Disease Study system for classifying age-related macular degeneration from stereoscopic color fundus photographs: the Age-Related Eye Disease Study Report Number 6. *American Journal of Ophthalmology*, *132*(5), 668–681.

Agnihotri, S. A., Mallikarjuna, N. N., & Aminabhavi, T. M. (2004). Recent advances on chitosan-based micro- and nanoparticles in drug delivery. *Journal of Controlled Release: Official Journal of the Controlled Release Society*, *100*(1), 5–28. doi:10.1016/j.jconrel.2004.08.010

Allegri, P., Mastromarino, A., & Neri, P. (2010). Management of chronic anterior uveitis relapses: efficacy of oral phospholipidic curcumin treatment. Long-term follow-up. *Clinical Ophthalmology (Auckland, N.Z.)*, *4*, 1201–1206. doi:10.2147/OPTH.S13271

Anand, P., Kunnumakkara, A., Newman, R., & Aggarwal, B. (2007). Bioavailability of Curcumin: Problems and Promises. *Molecular Phamaceutics*. 4(6), 807-818. doi: 10. 1021/mp700113r

Anitha, A., Maya, S., Deepa, N., Chennazhi, K. P., Nair, S. V., Tamura, H., & Jayakumar, R. (2011). Efficient water soluble O-carboxymethyl chitosan nanocarrier for the delivery of curcumin to cancer cells. *Carbohydrate Polymers*, *83*(2), 452–461. doi:10.1016/j.carbpol.2010.08.008

Arifin, D. R., & Palmer, A. F. (2003). Determination of size distribution and encapsulation efficiency of liposome-encapsulated hemoglobin blood substitutes using asymmetric flow field-flow fractionation coupled with multi-angle static

light scattering. *Biotechnology Progress*, *19*(6), 1798–1811. https://doi.org/10.1021/bp034120x

Avanti Polar Lipids, Inc. (2017). Lipid Products | 16:0 Liss Rhod PE | 810158. Retrieved from https://avantilipids.com/product/810158/

Avanti Polar Lipids. (2017). Mini-Extruder Extrusion Technique. Avanti Polar Lipids. Retrieved from https://avantilipids.com/divisions/equipment/mini-extruder-extrusion-technique/

Bagi, S. (n.d.). Human Eye Anatomy - Parts of the Eye Explained. Retrieved January 9, 2017, from http://www.allaboutvision.com/resources/anatomy.htm

Bajoria, R., Sooranna, S. R., & Contractor, S. F. (1997). Endocytotic uptake of small unilamellar liposomes by human trophoblast cells in culture. *Human reproduction*, *12*(6), 1343-1348.

Began, G., Sudharshan, E., Sankar, K. U., & Rao, A. G. (1999). Interaction of Curcumin with Phosphatidylcholine: A Spectrofluorometric Study. *Journal of Agricultural and Food Chemistry*, 47(12), 4992-4997. doi:10.1021/jf9900837

Beloqui, A., Memvanga, P. B., Coco, R., Reimondez-Troitiño, S., Alhouayek, M., Muccioli, G. G., … Préat, V. (2016). A comparative study of curcumin-loaded lipid-based nanocarriers in the treatment of inflammatory bowel disease. *Colloids and Surfaces B: Biointerfaces*, *143*, 327–335. https://doi.org/10.1016/j.colsurfb.2016.03.038

Bhawana, null, Basniwal, R. K., Buttar, H. S., Jain, V. K., & Jain, N. (2011). Curcumin nanoparticles: preparation, characterization, and antimicrobial study. *Journal of Agricultural and Food Chemistry*, *59*(5), 2056–2061. doi:10.1021/jf104402t

Binder, S., Stanzel, B. V., Krebs, I., & Glittenberg, C. (2007). Transplantation of the RPE in AMD. *Progress in Retinal and Eye Research*, *26*(5), 516–554. doi:10.1016/j.preteyeres.2007.02.002

Birke, K., Lipo, E., Birke, M. T., & Kumar-Singh, R. (2013). Topical Application of PPADS Inhibits Complement Activation and Choroidal Neovascularization in a Model of Age-Related Macular Degeneration. *PLoS ONE*, *8*(10), e76766. doi:10.1371/journal.pone.0076766

Bisht, S., Feldmann, G., Soni, S., Ravi, R., Karikar, C., Maitra, A., & Maitra, A. (2007). Polymeric nanoparticle-encapsulated curcumin ("nanocurcumin"): a novel strategy for human cancer therapy. *Journal of Nanobiotechnology*, *5*, 3. doi:10.1186/1477-3155-5-3

Calabrese, V., Bates, T. E., Mancuso, C., Cornelius, C., Ventimiglia, B., Cambria, M. T., Dinkova-Kostova, A. T. (2008). Curcumin and the cellular stress response in free radical-related diseases. *Molecular Nutrition & Food Research*, *52*(9), 1062–1073. doi:10.1002/mnfr.200700316

Chen, Y., Wu, Q., Zhang, Z., Yuan, L., Liu, X., & Zhou, L. (2012). Preparation of Curcumin-Loaded Liposomes and Evaluation of Their Skin Permeation and Pharmacodynamics. *Molecules*, 17(12), 5972-5987. doi:10.3390/molecules17055972

Choonara, Y. E., Pillay, V., Danckwerts, M. P., Carmichael, T. R., & du Toit, L. C. (2010). A review of implantable intravitreal drug delivery technologies for the treatment of posterior segment eye diseases. *Journal of Pharmaceutical Sciences*, *99*(5), 2219–2239. doi:10.1002/jps.21987

Curcio, C. A., Medeiros, N. E., & Millican, C. L. (1996). Photoreceptor loss in age-related macular degeneration. *Investigative Ophthalmology & Visual Science*, *37*(7), 1236–1249.

Dahan, A., & Miller, J. M. (2012). The solubility-permeability interplay and its implications in formulation design and development for poorly soluble drugs. *The AAPS Journal*, *14*(2), 244–251. doi:10.1208/s12248-012-9337-6

Dalle-Donne, I., Rossi, R., Giustarini, D., Milzani, A., & Colombo, R. (2003). Protein carbonyl groups as biomarkers of oxidative stress. *Clinica Chimica Acta*, *329*(1–2), 23–38. https://doi.org/10.1016/S0009-8981(03)00003-2

Dan, N. (2002). Effect of liposome charge and PEG polymer layer thickness on cell–liposome electrostatic interactions. *Biochimica et Biophysica Acta (BBA)-Biomembranes*, *1564*(2), 343-348.

Davis, B. M., Normando, E. M., Guo, L., Turner, L. A., Nizari, S., O'Shea, P., Cordeiro, M. F. (2014). Topical Delivery of Avastin to the Posterior Segment of the Eye In Vivo Using Annexin A5-associated Liposomes. *Small*, *10*(8), 1575–1584. doi:10.1002/smll.201303433

Demirbilek, S., Ersoy, M. O., Demirbilek, S., Karaman, A., Akin, M., Bayraktar, M., & Bayraktar, N. (2004). Effects of polyenylphosphatidylcholine on cytokines, nitrite/nitrate levels, antioxidant activity and lipid peroxidation in rats with sepsis. *Intensive Care Medicine*, *30*(10), 1974–1978. https://doi.org/10.1007/s00134-004-2234-4

Ding, X., Patel, M., & Chan, C. (2008). Molecular Pathology of Age-Related Macular Degeneration. *Progress in Retinal and Eye Research*. 28(1), 1-18.

https://doi.org/10.1016/j.preteyeres.2008.10.001

Düzgüneş, N., & Nir, S. (1999). Mechanisms and kinetics of liposome–cell interactions. *Advanced drug delivery reviews*, *40*(1), 3-18.Elouahabi, A., & Ruysschaert, J. M. (2005). Formation and intracellular trafficking of lipoplexes and polyplexes. *Molecular therapy*, *11*(3), 336-347.

Elouahabi, A., & Ruysschaert, J. M. (2005). Formation and intracellular trafficking of lipoplexes and polyplexes. *Molecular therapy*, *11*(3), 336-347.

Feng, S.-S., & Chien, S. (2003). Chemotherapeutic engineering: Application and further development of chemical engineering principles for chemotherapy of cancer and other diseases. *Chemical Engineering Science*, *58*(18), 4087–4114. https://doi.org/10.1016/S0009-2509(03)00234-3

Filipe, V., Hawe, A., & Jiskoot, W. (2010). Critical Evaluation of Nanoparticle Tracking Analysis (NTA) by NanoSight for the Measurement of Nanoparticles and Protein Aggregates. *Pharmaceutical Research*, *27*(5), 796–810. https://doi.org/10.1007/s11095-010-0073-2

Fiorentino, T. V., Prioletta, A., Zuo, P., & Folli, F. (2013). Hyperglycemia-induced oxidative stress and its role in diabetes mellitus related cardiovascular diseases. *Current Pharmaceutical Design*, *19*(32), 5695–5703.

Gerson, J. D. (2009). Costs of treatment for age-related macular degeneration. *Optometry (St. Louis, Mo.)*, *80*(7), 339.

Ghyczy, M., Torday, C., Kaszaki, J., Szabó, A., Czóbel, M., & Boros, M. (2008). Oral phosphatidylcholine pretreatment decreases ischemia-reperfusion-induced methane generation and the inflammatory response in the small intestine. *Shock*

(Augusta, Ga.), *30*(5), 596–602. https://doi.org/10.1097/SHK.0b013e31816f204

Giannaccini, M., Giannini, M., Calatayud, M. P., Goya, G. F., Cuschieri, A., Dente, L., & Raffa, V. (2014). Magnetic Nanoparticles as Intraocular Drug Delivery System to Target Retinal Pigmented Epithelium (RPE). *International Journal of Molecular Sciences*, *15*(1), 1590–1605. doi:10.3390/ijms15011590

Gicquaud, C., Chauvet, J.-P., & Tancrède, P. (2003). Surface film pressure of actin: interactions with lipids in mixed monolayers. *Biochemical and Biophysical Research Communications*, *308*(4), 995–1000.

Glover, D. J., Glouchkova, L., Lipps, H. J., & Jans, D. A. (2007). Overcoming barriers to achieve safe, sustained and efficient non-viral gene therapy. *Adv Gene Mol Cell Ther*, *1*(2), 126-140.

Gomes, M. J., Neves, J. das, & Sarmento, B. (2014). Nanoparticle-based drug delivery to improve the efficacy of antiretroviral therapy in the central nervous system. *International Journal of Nanomedicine*, *9*, 1757–1769. doi:10.2147/IJN.S45886

Graf, E., & Penniston, J. T. (1980). Method for determination of hydrogen peroxide, with its application illustrated by glucose assay. *Clinical Chemistry*, *26*(5), 658–660.

Grama, C. N., Suryanarayana, P., Patil, M. A., Raghu, G., Balakrishna, N., Kumar, M. N. V. R., & Reddy, G. B. (2013). Efficacy of Biodegradable Curcumin Nanoparticles in Delaying Cataract in Diabetic Rat Model. *PLoS ONE*, *8*(10), e78217. doi:10.1371/journal.pone.0078217

Hamidi, M., Azadi, A., & Rafiei, P. (2008). Hydrogel nanoparticles in drug delivery. *Advanced Drug Delivery Reviews*, *60*(15), 1638–1649.

doi:10.1016/j.addr.2008.08.002

Hironaka, K., Inokuchi, Y., Fujisawa, T., Shimazaki, H., Akane, M., Tozuka, Y., … Takeuchi, H. (2011). Edaravone-loaded liposomes for retinal protection against oxidative stress-induced retinal damage. *European Journal of Pharmaceutics and Biopharmaceutics*, *79*(1), 119–125. doi:10.1016/j.ejpb.2011.01.019

Hollborn, M., Chen, R., Wiedemann, P., Reichenbach, A., Bringmann, A., & Kohen, L. (2013). Cytotoxic Effects of Curcumin in Human Retinal Pigment Epithelial Cells. *PLoS ONE*, *8*(3), e59603. doi:10.1371/journal.pone.0059603

Honary, S., & Zahir, F. (2013). Effect of zeta potential on the properties of nano-drug delivery systems-a review (Part 1). *Tropical Journal of Pharmaceutical Research*, *12*(2), 255-264.

Hudson, H. L., Stulting, R. D., Heier, J. S., Lane, S. S., Chang, D. F., Singerman, L. J., Leonard, R. E. (2008). Implantable Telescope for End-Stage Age-related Macular Degeneration: Long-term Visual Acuity and Safety Outcomes. American Journal of Ophthalmology, 146(5), 664–673.e1. https://doi.org/10.1016/j.ajo.2008.07.003

Jawahar, N., & Meyyanathan, S. N. (2012). Polymeric nanoparticles for drug delivery and targeting: A comprehensive review. *International Journal of Health & Allied Sciences*, *1*(4), 217. https://doi.org/10.4103/2278-344X.107832

Jia, L., Dong, Y., Yang, H., Pan, X., Fan, R., & Zhai, L. (2011). Serum superoxide dismutase and malondialdehyde levels in a group of Chinese patients with age-related macular degeneration. *Aging Clinical and Experimental Research*, *23*(4), 264–267.

Jithan, A., Madhavi, K., Madhavi, M., & Prabhakar, K. (2011). Preparation and

characterization of albumin nanoparticles encapsulating curcumin intended for the treatment of breast cancer. *International Journal of Pharmaceutical Investigation*, *1*(2), 119–125. doi:10.4103/2230-973X.82432

Jitsanong, T., Khanobdee, K., Piyachaturawat, P., & Wongprasert, K. (2011). Diarylheptanoid 7-(3,4 dihydroxyphenyl)-5-hydroxy-1-phenyl-(1E)-1-heptene from Curcuma comosa Roxb. protects retinal pigment epithelial cells against oxidative stress-induced cell death. *Toxicology in Vitro*, *25*(1), 167–176. https://doi.org/10.1016/j.tiv.2010.10.014

Kang, J. H., Jang, W. Y., & Ko, Y. T. (2017). The Effect of Surface Charges on the Cellular Uptake of Liposomes Investigated by Live Cell Imaging. *Pharmaceutical Research*, 1-14.

Kansara, V., & Mitra, A. K. (2006). Evaluation of an ex vivo model implication for carrier-mediated retinal drug delivery. *Current Eye Research*, *31*(5), 415–426. doi:10.1080/02713680600646890

Kant, V., Gopal, A., Pathak, N. N., Kumar, P., Tandan, S. K., & Kumar, D. (2014). Antioxidant and anti-inflammatory potential of curcumin accelerated the cutaneous wound healing in streptozotocin-induced diabetic rats. *International Immunopharmacology*, *20*(2), 322–330. https://doi.org/10.1016/j.intimp.2014.03.009

Karam, S. H., Issa, H. I., Mohamed, A. S., & Hassanin, O. A. (2014). Nicotine, curcumin, and cornea: an experimental histopathological study. Egyptian Journal of Pathology, 34(1), 39–43. https://doi.org/10.1097/01.XEJ.0000446918.03067.c7

Karewicz, A., Bielska, D., Gzyl-Malcher, B., Kepczynski, M., Lach, R., & Nowakowska,

M. (2011). Interaction of curcumin with lipid monolayers and liposomal bilayers. *Colloids and Surfaces B: Biointerfaces*, *88*(1), 231–239. https://doi.org/10.1016/j.colsurfb.2011.06.037

Kaskoos, R. A. (2014). Investigation of moxifloxacin loaded chitosan–dextran nanoparticles for topical instillation into eye: In-vitro and ex-vivo evaluation. *International Journal of Pharmaceutical Investigation*, *4*(4), 164–173. https://doi.org/10.4103/2230-973X.143114

Kaur, I. P., & Kakkar, S. (2014). Nanotherapy for posterior eye diseases. *Journal of Controlled Release: Official Journal of the Controlled Release Society*, *193*, 100–112. doi:10.1016/j.jconrel.2014.05.031

Kim, M.-H., Chung, J., Yang, J., Chung, S.-M., Kwag, N.-H., & Yoo, J.-S. (2003). Hydrogen peroxide-induced cell death in a human retinal pigment epithelial cell line, ARPE-19. *Korean Journal of Ophthalmology: KJO*, *17*(1), 19–28. https://doi.org/10.3341/kjo.2003.17.1.19

Kohen, R., & Nyska, A. (2002). Oxidation of Biological Systems: Oxidative Stress Phenomena, Antioxidants, Redox Reactions, and Methods for Their Quantification. *Toxicologic Pathology*,30(6), 620-650. doi:10.1080/0192623029016672 4

Kubinyi, H. (1979). Nonlinear dependence of biological activity on hydrophobic character: the bilinear model. *Il Farmaco; Edizione Scientifica*, *34*(3), 248–276.

Kunwar, A., Barik, A., Pandey, R., & Priyadarsini, K. I. (2006). Transport of liposomal and albumin loaded curcumin to living cells: An absorption and fluorescence spectroscopic study. *Biochimica et Biophysica Acta (BBA) - General Subjects*,

1760(10), 1513–1520. doi:10.1016/j.bbagen.2006.06.012

Kunwar, A., Barik, A., Priyadarsini, K., & Pandey, R. (2007). Absorption and fluorescence studies of curcumin bound to liposome and living cells. *BARC Newsletter*, (285), 213–219.

Lee, H. S., Kim, B. K., Nam, Y., Sohn, U. D., Park, E. S., Hong, S. A., … Jeong, J. H. (2013). Protective role of phosphatidylcholine against cisplatin-induced renal toxicity and oxidative stress in rats. *Food and Chemical Toxicology*, *58*, 388–393. https://doi.org/10.1016/j.fct.2013.05.005

Lee, S., Ashizawa, A. T., Kim, K. S., Falk, D. J., & Notterpek, L. (2013). Liposomes to target peripheral neurons and Schwann cells. *PloS one*, *8*(11), e78724

Liang, X., Mao, G., & Ng, K. S. (2004). Mechanical properties and stability measurement of cholesterol-containing liposome on mica by atomic force microscopy. *Journal of Colloid and Interface Science*, *278*(1), 53-62.

Lim, L. S., Mitchell, P., Seddon, J. M., Holz, F. G., & Wong, T. Y. (2012). Age-related macular degeneration. *The Lancet*, *379*(9827), 1728–1738. doi:10.1016/S0140-6736(12)60282-7

Liu, B., Wang, Q., Yu, S., Zhao, T., Han, J., Jing, P., … Yan, C.-H. (2013). Double shelled hollow nanospheres with dual noble metal nanoparticle encapsulation for enhanced catalytic application. *Nanoscale*, *5*(20), 9747–9757. doi:10.1039/C3NR02759G

Loftsson, T., & Stefánsson, E. (2002). Cyclodextrins in eye drop formulations: enhanced topical delivery of corticosteroids to the eye. *Acta Ophthalmologica Scandinavica*, *80*(2), 144–150. doi:10.1034/j.1600-0420.2002.800205.x

Mahfouz, M., & Kummerow, F. (2000). Cholesterol-rich diets have different effects on lipid peroxidation, cholesterol oxides, and antioxidant enzymes in rats and rabbits. *The Journal of Nutritional Biochemistry.* 11(5), 293-302. https://doi.org/10.1016/S0955-2863(00)00083-8

Malvern Instruments. (2004). Zetasizer Nano Series User Manual. Malvern Instruments Ltd, Malvern, Worcestershire, United Kingdom. Retrieved from http://www.biophysics.bioc.cam.ac.uk/files/Zetasizer_Nano_user_manual_Man0317-1.1.pdf

Mandal, M. N. A., Patlolla, J. M. R., Zheng, L., Agbaga, M.-P., Tran, J.-T. A., Wicker, L., … Anderson, R. E. (2009). Curcumin protects retinal cells from light-and oxidant stress-induced cell death. *Free Radical Biology and Medicine*, *46*(5), 672–679. doi:10.1016/j.freeradbiomed.2008.12.006

Mangolim, C. S., Moriwaki, C., Nogueira, A. C., Sato, F., Baesso, M. L., Neto, A. M., & Matioli, G. (2014). Curcumin–β-cyclodextrin inclusion complex: Stability, solubility, characterisation by FT-IR, FT-Raman, X-ray diffraction and photoacoustic spectroscopy, and food application. *Food Chemistry*, *153*, 361–370. https://doi.org/10.1016/j.foodchem.2013.12.067

Marczylo, T. H., Verschoyle, R. D., Cooke, D. N., Morazzoni, P., Steward, W. P., & Gescher, A. J. (2007). Comparison of systemic availability of curcumin with that of curcumin formulated with phosphatidylcholine. *Cancer Chemotherapy and Pharmacology*, *60*(2), 171–7. doi:http://dx.doi.org/10.1007/s00280-006-0355-x

Mazzolani, F. (2012). Pilot study of oral administration of a curcumin-phospholipid formulation for treatment of central serous chorioretinopathy. *Clinical*

Ophthalmology (Auckland, N.Z.), *6*, 801–806. doi:10.2147/OPTH.S31859

McNally, S. J., Harrison, E. M., Ross, J. A., Garden, O. J., & Wigmore, S. J. (2007). Curcumin induces heme oxygenase 1 through generation of reactive oxygen species, p38 activation and phosphatase inhibition. *International Journal of Molecular Medicine*, *19*(1), 165–172.

Meerovich, K. V., Meerovich, G., Lukyanets, E., Negrimovsky, V., Barkanova, S., Umnova, L., & Loschenov, V. (2008). New Efficient Nanostructural Near-IR Photosensitizer for Photodynamic Therapy of Malignancies based on Micellar Dispersion of Zinc octa-4,5-decylthio-octa-3,6-chlorophthalocyanine. *Nano Science and Technology Institute*, *2*.

Mirza, M., Volz, C., Karlstetter, M., Langiu, M., Somogyi, A., Ruonala, M. O., … Langmann, T. (2013). Progressive Retinal Degeneration and Glial Activation in the CLN6nclf Mouse Model of Neuronal Ceroid Lipofuscinosis: A Beneficial Effect of DHA and Curcumin Supplementation. *PLoS ONE*, *8*(10), 1–11. doi:10.1371/journal.pone.0075963

Moghaddam, B., Ali, M. H., Wilkhu, J., Kirby, D. J., Mohammed, A. R., Zheng, Q., & Perrie, Y. (2011). The application of monolayer studies in the understanding of liposomal formulations. *International Journal of Pharmaceutics*, *417*(1), 235-244.

Molina-Jijón, E., Tapia, E., Zazueta, C., El Hafidi, M., Zatarain-Barrón, Z. L., Hernández-Pando, R., … Pedraza-Chaverri, J. (2011). Curcumin prevents Cr(VI)-induced renal oxidant damage by a mitochondrial pathway. *Free Radical Biology and Medicine*, *51*(8), 1543–1557. doi:10.1016/j.freeradbiomed.2011.07.018

National Academy of Sciences. (2015). Advancing Therapeutic Development for Dry

Age-Related Macular Degeneration (AMD): Workshop in Brief. *Institute of Medicine of the National Academies.* 1-8.

National Eye Institute. (2013). Facts About Age-Related Macular Degeneration. Retrieved from https://www.nei.nih.gov/health/maculardegen/armd_facts

Nguyen, J., Xie, X., Neu, M., Dumitrascu, R., Reul, R., Sitterberg, J., Kissel, T. (2008). Effects of cell-penetrating peptides and pegylation on transfection efficiency of polyethylenimine in mouse lungs. *The Journal of Gene Medicine*, *10*(11), 1236–1246. doi:10.1002/jgm.1255

Park, J. W., Hong, K., Kirpotin, D. B., Colbern, G., Shalaby, R., Baselga, J., Benz, C. C. (2002). Anti-HER2 Immunoliposomes Enhanced Efficacy Attributable to Targeted Delivery. *Clinical Cancer Research*, *8*(4), 1172–1181.

Peetla, C., Stine, A., & Labhasetwar, V. (2009). Biophysical Interactions with Model Lipid Membranes: Applications in Drug Discovery and Drug Delivery. *Molecular Pharmaceutics*, *6*(5), 1264–1276. https://doi.org/10.1021/mp9000662

Pescosolido, N., Giannotti, R., Plateroti, A. M., Pascarella, A., & Nebbioso, M. (2014). Curcumin: therapeutical potential in ophthalmology. *Planta Medica*, *80*(4), 249–254. doi:10.1055/s-0033-1351074

Peyman, G. A., Schulman, J. A., & Neisman, M. R. (1995). Uptake of liposomes by human retinal pigment epithelial cells in culture. In *Biomedical Engineering Conference, 1995., Proceedings of the 1995 Fourteenth Southern* (p. 125). IEEE.

Porte, C. (2012). Pathogenesis and management of age related macular degeneration. *Scottish Universities Medical Journal*. 1(2); 141-153.

Preetha, A., Huilgol, N., & Banerjee, R. (2006). Comparison of paclitaxel penetration in

normal and cancerous cervical model monolayer membranes. *Colloids and Surfaces B: Biointerfaces*, *53*(2), 179–186. https://doi.org/10.1016/j.colsurfb.2006.09.005

Puri, A., Jang, H., Yavlovich, A., Masood, M. A., Veenstra, T. D., Luna, C., Blumenthal, R. (2011). Material properties of matrix lipids determine the conformation and intermolecular reactivity of diacetylenic phosphatidylcholine in the lipid bilayer. *Langmuir: The ACS Journal of Surfaces and Colloids*, *27*(24), 15120–15128. https://doi.org/10.1021/la203453x

Prasad, S., & Aggarwal, B. B. (2011). Turmeric, the Golden Spice: From Traditional Medicine to ModerElouahabi, A., & Ruysschaert, J. M. (2005). Formation and intracellular trafficking of lipoplexes and polyplexes. *Molecular therapy*, *11*(3), 336-347.n Medicine. In I. F. F. Benzie & S. Wachtel-Galor (Eds.), *Herbal Medicine: Biomolecular and Clinical Aspects* (2nd ed.). Boca Raton (FL): CRC Press/Taylor & Francis. Retrieved from http://www.ncbi.nlm.nih.gov/books/NBK92752/

Quellec, G., Russell, S. R., & Abramoff, M. D. (2011). Optimal Filter Framework for Automated, Instantaneous Detection of Lesions in Retinal Images. *IEEE Transactions on Medical Imaging*, *30*(2), 523–533. doi:10.1109/TMI.2010.2089383

Rampino, A., Borgogna, M., Blasi, P., Bellich, B., & Cesàro, A. (2013). Chitosan nanoparticles: preparation, size evolution and stability. *International Journal of Pharmaceutics*, *455*(1-2), 219–228. doi:10.1016/j.ijpharm.2013.07.034

Redmond, T.M., Yu, S., Lee, E., Bok, D., Hamasaki, D., Chen, N., Goletz, P., Ma, J.-X., Crouch, R.K. and Pfeiffer, K.: *Rpe65* is necessary for production of 11-*cis*-

Vitamin A in the retinal visual cycle. *Nature Genetics* 20: 344-350, 1998.

Rosenfeld, P. J., Brown, D. M., Heier, J. S., Boyer, D. S., Kaiser, P. K., Chung, C. Y., MARINA Study Group. (2006). Ranibizumab for neovascular age-related macular degeneration. *The New England Journal of Medicine*, *355*(14), 1419–1431. doi:10.1056/NEJMoa054481

Salem, N. A., Abdel-Rahman, G. M., Ewias, M., & Tsegay, A. T. (2012). Effects of Curcumin on Early Retinal Neuro-Degenerative Changes in Diabetic Albino Rats. *The Journal of American Science*, *8*(1), 435–444.

Sanger, J. W., Mittal, B., & Sanger, J. M. (1984). Interaction of fluorescently-labeled contractile proteins with the cytoskeleton in cell models. *The Journal of Cell Biology*, *99*(3), 918–928.

Sasaki, H., Karasawa, K., Hironaka, K., Tahara, K., Tozuka, Y., & Takeuchi, H. (2013). Retinal drug delivery using eyedrop preparations of poly-l-lysine-modified liposomes. *European Journal of Pharmaceutics and Biopharmaceutics*, *83*(3), 364–369. doi:10.1016/j.ejpb.2012.10.014

Schieber, M., & Chandel, N. S. (2014). ROS function in redox signaling and oxidative stress. *Current Biology*, *24*(10), R453-R462.

Shaikh, J., Ankola, D. D., Beniwal, V., Singh, D., & Kumar, M. N. V. R. (2009). Nanoparticle encapsulation improves oral bioavailability of curcumin by at least 9-fold when compared to curcumin administered with piperine as absorption enhancer. *European Journal of Pharmaceutical Sciences*, *37*(3–4), 223–230. doi:10.1016/j.ejps.2009.02.019

Sharma, N., Gupta, A., Prabhakar, S., Singh, R., Sharma, S., & Anand, A. (2013).

Association of the SOD activity, rs1061170 in CFH and rs1531289 in VEGFR2 with protein levels in North Indian age related macular degeneration patients. *Investigative Ophthalmology & Visual Science*, *54*(15), 6190–6190.

Snodderly, D. M. (1995). Evidence for protection against age-related macular degeneration by carotenoids and antioxidant vitamins. *The American Journal of Clinical Nutrition*, *62*(6), 1448S.

Soenen, S. J., Brisson, A. R., & De Cuyper, M. (2009). Addressing the problem of cationic lipid-mediated toxicity: the magnetoliposome model. *Biomaterials*, *30*(22), 3691-3701.

Spaide, R. F., Sorenson, J., & Maranan, L. (2003). Combined photodynamic therapy with verteporfin and intravitreal triamcinolone acetonide for choroidal neovascularization. *Ophthalmology*, *110*(8), 1517–1525. https://doi.org/10.1016/S0161-6420(03)00544-X

Straubinger, R. M., Hong, K., Friend, D. S., & Papahadjopoulos, D. (1983). Endocytosis of liposomes and intracellular fate of encapsulated molecules: encounter with a low pH compartment after internalization in coated vesicles. *Cell*, *32*(4), 1069-1079.

Takahashi, M., Uechi, S., Takara, K., Asikin, Y., & Wada, K. (2009). Evaluation of an Oral Carrier System in Rats: Bioavailability and Antioxidant Properties of Liposome-Encapsulated Curcumin. *Journal of Agricultural and Food Chemistry*, 57(19), 9141-9146. doi:10.1021/jf9013923

Taylor, R., Coulombe, S., Otanicar, T., Phelan, P., Gunawan, A., Lv, W., Tyagi, H. (2013). Small particles, big impacts: A review of the diverse applications of

nanofluids. *Journal of Applied Physics*, *113*(1), 011301–011301–19. doi:10.1063/1.4754271

Thermo Fisher Scientific. (2008). NanoDrop 1000 Spectrophotometer V3.7 User's Manual. Thermo Fisher Scientific. Retrieved from http://www.nanodrop.com/library/nd-1000-v3.7-users-manual-8.5x11.pdf

Totan, Y., Yağcı, R., Bardak, Y., Özyurt, H., Kendir, F., Yılmaz, G., Tığ, U. Ş. (2009). Oxidative Macromolecular Damage in Age-Related Macular Degeneration. *Current Eye Research*, *34*(12), 1089–1093. doi:10.3109/02713680903353772

Weydert, C. J., & Cullen, J. J. (2010). Measurement of superoxide dismutase, catalase and glutathione peroxidase in cultured cells and tissue. *Nature protocols*, *5*(1), 51-66.

Wong, W. L., Su, X., Li, X., Cheung, C. M. G., Klein, R., Cheng, C.-Y., & Wong, T. Y. (2014). Global prevalence of age-related macular degeneration and disease burden projection for 2020 and 2040: a systematic review and meta-analysis. *The Lancet Global Health*, *2*(2), e106–e116. doi:10.1016/S2214-109X(13)70145-1

Woo, J. M., Shin, D.-Y., Lee, S. J., Joe, Y., Zheng, M., Yim, J. H., Chung, H. T. (2012). Curcumin protects retinal pigment epithelial cells against oxidative stress via induction of heme oxygenase-1 expression and reduction of reactive oxygen. *Molecular Vision*, *18*, 901–908.

Xuan, B., McClellan, D. a., Moore, R., & Chiou, G. c. y. (2005). Alternative Delivery of Insulin via Eye Drops. *Diabetes Technology & Therapeutics*, *7*(5), 695–698. doi:10.1089/dia.2005.7.695

Yadav, V. R., Suresh, S., Devi, K., & Yadav, S. (2009). Effect of Cyclodextrin

Complexation of Curcumin on its Solubility and Antiangiogenic and Anti-inflammatory Activity in Rat Colitis Model. *AAPS PharmSciTech*, *10*(3), 752–762. doi:10.1208/s12249-009-9264-8

Yildirim, Z., Ucgun, N. I., & Yildirim, F. (2011). The role of oxidative stress and antioxidants in the pathogenesis of age-related macular degeneration. *Clinics*, *66*(5), 743–746. https://doi.org/10.1590/S1807-59322011000500006

Ying, L., Tahara, K., & Takeuchi, H. (2013). Drug delivery to the ocular posterior segment using lipid emulsion via eye drop administration: Effect of emulsion formulations and surface modification. *International Journal of Pharmaceutics*, *453*(2), 329–335. doi:10.1016/j.ijpharm.2013.06.024

Yuan, Y., & Kitts, D. (2003). Dietary (n-3) Fat and Cholesterol Alter Tissue Antioxidant Enzymes and Susceptibility to Oxidation in SHR and WKY Rats. *The Journal of Nutrition.* 133(3), 679-688.

Yuan, Y., Kitts, D., & Godin, D. (1998). Variations in Dietary Fat and Cholesterol Intakes Modify Antioxidant Status of SHR and WKY Rats. *The Journal of Nutrition.* 128(10), 1620-1630.

Zhao, L., & Feng, S.-S. (2006). Effects of cholesterol component on molecular interactions between paclitaxel and phospholipid within the lipid monolayer at the air–water interface. *Journal of Colloid and Interface Science*, *300*(1), 314–326. https://doi.org/10.1016/j.jcis.2006.03.035

Zingg, J. M., Hasan, S. T., Cowan, D., Ricciarelli, R., Azzi, A., & Meydani, M. (2012). Regulatory effects of curcumin on lipid accumulation in monocytes/macrophages. *Journal of cellular biochemistry*, *113*(3), 833-840.

Appendix A: Glossary

Absorption Spectrophotometer - instrument used to measure the ability of certain molecules to absorb particular wavelengths

Amphiphilic - used to describe a compound that has both lipid-based and water-based properties

Angiogenesis - process where new blood vessels are created from pre-existing vessels

Antioxidants - a molecule that inhibits oxidation of other molecules; reduces oxidative stress

Bioavailability - how fast or how much of a substance is absorbed by a living system

Choroid - connective tissue layer between retina and sclera in the eye

Drusen - yellow deposits under the retina

Lysate - preparation of a product of cells, such as protein, DNA, or RNA

Oxidative stress - a result of the imbalance between reactive oxygen species and the body's ability to detoxify it

Nanoliposome (NL) - synthesized submicron vesicle composed of a lipid bilayer used in drug delivery

Phosphatidylcholine (PC) - type of phospholipid that is a major component in liposome membranes

Retinal pigment epithelium (RPE) - layer of cells that are located between the choriocapillaris and outer segments of the photoreceptors; interacts with these photoreceptors to maintain vision

Retinoprotective - the ability to protect the retina from degeneration; can occur, for example, by decreasing the oxidative stress of cells in the retina

Vascular endothelial growth factor (VEGF) - a signal protein; responsible for stimulating angiogenesis and vasculogenesis

Vasculogenesis - process in which new blood vessels are created where there are not pre-existing vessels

Appendix B: Curcumin Structure

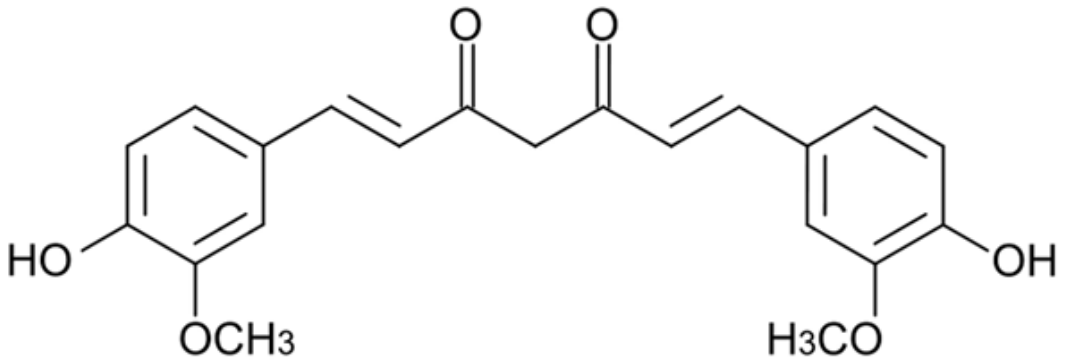

Curcumin, 1,3-diketo form. Source: AVA Plant Co., Ltd. (2011). Aquacumin – Water Soluble Curcumin. Retrieved from http://www.avaplant.com/products/semi-finished-material/water-soluble-curcumin/

Appendix C: Franz Diffusion Cell

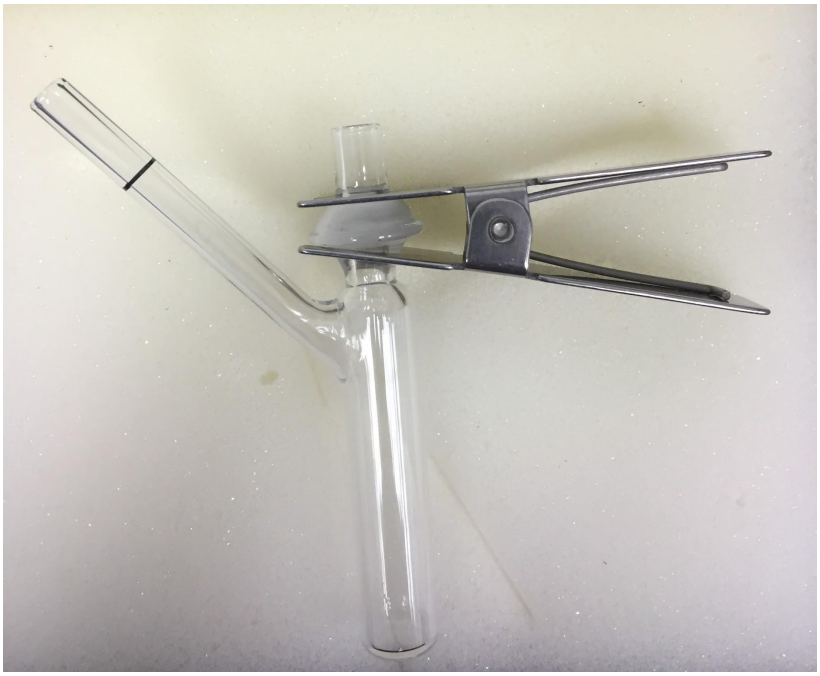

Photograph of the 5 mm clear unjacketed Franz diffusion cell with 12 mm outer diameter spherical joint and 5 mL receptor volume used for *ex vivo* testing. Photograph taken by Team INJECT.

Appendix D: Standard Curve of Curcumin in Sucrose

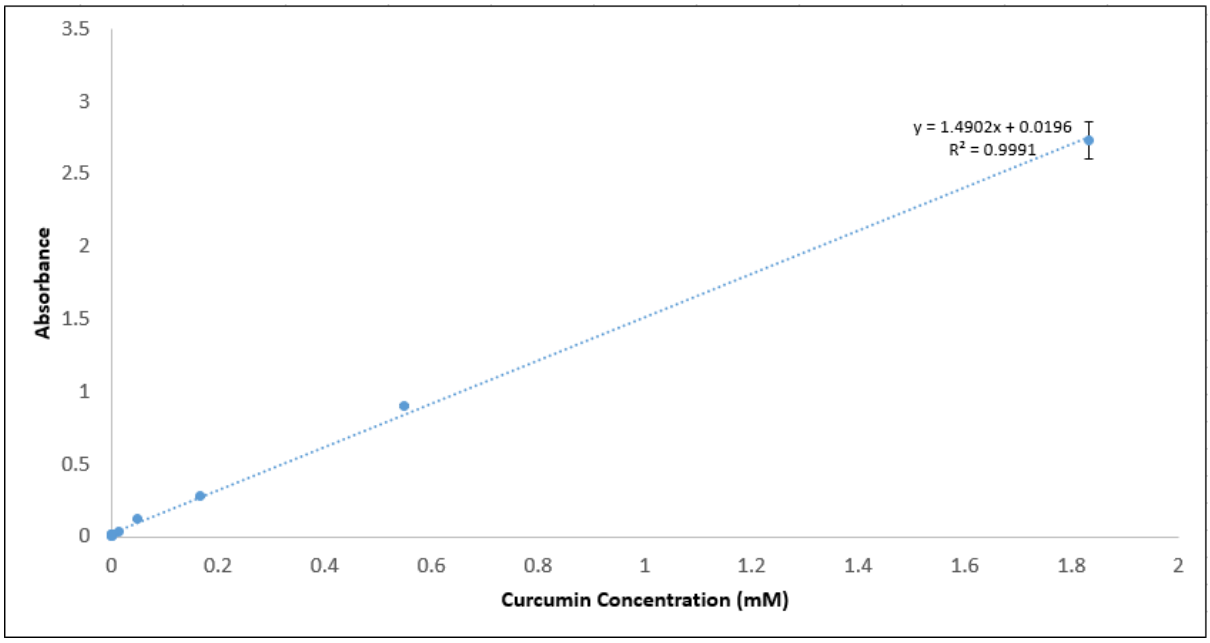

A standard curve of curcumin in sucrose was created by plotting absorbance vs curcumin concentration. Fifteen data points between 1 nM and 2 mM were plotted.

Appendix E: Langmuir Trough Monolayer Experiments

Volumes of phosphatidylcholine (PC), cholesterol (C), and curcumin (Cur) used to prepare each mixture. In all mixtures, the total lipid (PC+C) to curcumin ratio was kept at a 1:1 molar ratio.

Mixture	Total (µL)	PC (µL)	C (µL)	Cur (µL)
4:1 PC/C	3.38	2.71	0.677	--
4:1 PC/C/Cur	5	2.71	0.677	1.61
1:1 PC/C	1.7	0.85	0.85	--
1:1 PC/C/Cur	2.51	0.85	0.85	0.81
PC	3	3	--	--
PC/Cur	4.43	3	--	1.43

Appendix F: Nanoliposome Preparation

1. Pipette 76 μL of 32.46 mM phosphatidylcholine solution, 19 μL of 32.46 mM cholesterol solution, 45.4 μL of 25 mg/mL curcumin stock, and 2.12 μL of lissamine rhodamine B solution into a Fisherbrand™ Class B Clear Glass Threaded Vial to achieve a 1:1 ratio of total lipid: curcumin, with a 4:1 ratio of phosphatidylcholine: cholesterol. To prepare empty NL, add the same volumes of just the phosphatidylcholine, cholesterol, and lissamine rhodamine B solutions.
2. Layer NL solution against the walls of the vial by slowly rotating the vial horizontally for 60 seconds.
3. Remove the excess solvent through evaporation by placing the glass vial in a vacuum chamber for at least 3 hours.
4. Rehydrate the dry lipid film with 1 mL sucrose.
5. Store the vials at 4 °C overnight to allow for the self-assembly of the NL complex.
6. Assemble mini-extruder according to the manufacturer's use instructions, using 200 μM filters.
7. Extrude the NL complex solution by passing through the extruder 10 times.

Appendix G: Nanoliposome Viewing Chamber Preparation and Imaging Protocol

1. Form a viewing chamber by coating two opposite sides of a square glass coverslip with vacuum grease and placing it gently on a microscope slide, leaving a small gap between the uncoated sides of the coverslip and the slide.
2. Pipette 90 μL of glucose solution through the gap and into the middle of the coverslip-slide area.
3. Extract 10 μL from the top of the NL solution (where there is a greater concentration of particles) and pipette it the opening and into middle of the glucose solution.
4. Allow the NL solution to spread throughout the viewing chamber to allow for uniform imaging.
5. Image NL under brightfield and FITC filters.

Appendix H: Nanodrop (UV-Vis Spectroscopy) Protocol

Adapted from NanoDrop 1000 Spectrophotometer V3.7 User's Manual (Thermo Fisher Scientific)

1. Clean both the upper and lower pedestals of the sample retention system with 2 µl deionized water aliquots and a laboratory wipe. (If decontamination is necessary, use 2 µL aliquots of 0.5% sodium hypochlorite solution).
2. Set the absorbance wavelength for 416 nm for curcumin detection.
3. Pipette 2 µL of blank solution onto the lower pedestal, lower the lever, and press 'Blank'.
4. After measurement has been taken, lift the lever and clean the pedestal of the blank solution using a laboratory wipe.
5. Pipette 2 µL of experimental solution onto the lower pedestal. Lower lever and press 'Measure'.
6. After measurement has been taken, lift the lever and clean the pedestal of the experimental solution using a laboratory wipe.
7. After all measurements have been taken and data recorded, pipette 2 µL of deionized water onto both the upper and lower pedestals and clean with a laboratory wipe.

Appendix I: Nanosight Nanoliposome Size Distribution Protocol

1. Pipette 400-500 μL of sample or sample dilution into using a 1 mL disposable syringe into the platform.
2. Turn on the machinery and the Nanosight software.
3. Press ‘Capture’ within the software and focus the image to find a vertical red line on the screen.
4. Image to the left of the red line so that one peak appears on the output and there is less red within the viewing screen. (If image is unsatisfactory: filter or dilute the sample.)
5. Click ‘Record’.

Appendix J: MTT Assay Reagent Reconstitution

Protocol adapted from Caymen Chemical's MTT Cell Proliferation Assay Kit

I. Assay buffer preparation - Prepared by dissolving the Cell-Based Buffer Tablet in 100 mL of distilled water
II. MTT Reagent - Prepared by dissolving the MTT Reagent in 5 mL of Assay Buffer
III. Crystal Dissolving Solution - Prepared by dissolving the Crystal Dissolving SDS powder with Crystal Dissolving hydrochloride

Chemical Reaction for MTT Assay

This assay operates on the principle of reducing MTT to formazan. MTT is uptaken into the cell and reduced by oxioreductases in the cell. Therefore, a high formazan level indicates a high metabolic activity level

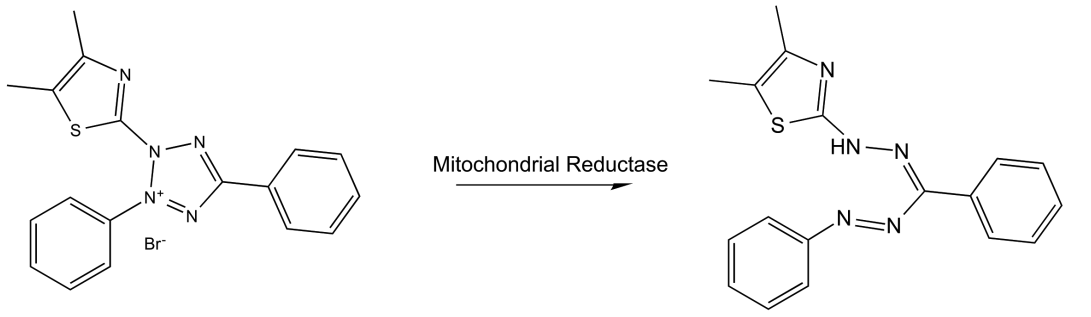

3-(4,5-dimethylthiazol-2-yl)-2,5-diphenyltetrazolium bromide **(MTT)**

(*E*,*Z*)-5-(4,5-dimethylthiazol-2-yl)-1,3-diphenylformazan **(Formazan)**

From:
https://upload.wikimedia.org/wikipedia/commons/thumb/d/de/MTT_reaction.png/500px-MTT_reaction.png

Appendix K: ROS Assay Reagent Reconstitution

Protocol adapted from Cell BioLab's Reactive Oxygen Species Assay kit.

I. Dye Preparation - The DCFH-DA dye was prepared by diluting the 20X stock to 1X in DMEM basal media

Chemical Reaction for ROS Assay

The ROS assay involves the measurement of the DCF dye. Cells initially uptake a nonfluorescent molecule, DCFH-DA, which then permeates the cell membrane. When this molecule reacts with radical species, it reduces to the fluorescent molecule DCF. From: http://www.cellbiolabs.com/sites/default/files/STA-342%20Fig%201.jpg